

Molecular composition and processing of aqueous secondary organic aerosol in ~~cloud~~clouds at a mountain site in southeastern China

Yali Jin^{1,2,3,4}, Hao Luo^{1,6}, Siqu Tang¹, Shuhui Xue¹, Chengyu Nie¹, Xiacong Peng³Peng⁷, Yan Zheng⁹, Weiqi Xu⁷Xu⁸, Guohua Zhang⁷, Xiaole Pan⁸, Yele Sun⁸, Qi Chen⁹, Lanzhong Liu⁸, and Defeng Zhao^{1,3,4,5}

5 ¹Department of Atmospheric and Oceanic Sciences & Institute of Atmospheric Sciences, Fudan University, Shanghai, 200438, China

²Shanghai Frontiers Science Center of Atmosphere-Ocean Interaction, Fudan University, Shanghai, 200438, China

³Shanghai Key Laboratory of Ocean-land-atmosphere Boundary Dynamics and Climate Change, Fudan University, Shanghai, 200438, China

10 ⁴National Observations and Research Station for Wetland Ecosystems of the Yangtze Estuary, Fudan University, Shanghai, 200438, China

⁵Institute of Eco-Chongming (IEC), 20 Cuiniao Rd., Chongming, Shanghai, 202162, China

⁶Inner Mongolia Key Laboratory of Pollution Control and Low Carbon Resource Utilization, Inner Mongolia University, Inner Mongolia, 010021, China

15 ⁷State Key Laboratory of Advanced Environmental Technology, Guangzhou Institute of Geochemistry, Chinese Academy of Sciences, Guangzhou, 510640, China

⁸State Key Laboratory of Atmospheric Environment and Extreme Meteorology, Institute of Atmospheric Physics, Chinese Academy of Sciences, Beijing, 100029, China

20 ⁹State Key Laboratory of Regional Environment and Sustainability, College of Environmental Sciences and Engineering, Peking University, Beijing, 100871, China

Corresponding to: Defeng Zhao (dfzhao@fudan.edu.cn)

Abstract. Aqueous secondary organic aerosol (aqSOA) contributes substantially to organic aerosol (OA), affecting air quality, human health, and climate. However, the molecular composition and processing of aqSOA in ~~clouds~~ remain unclear due to limited online field measurements. We measured molecular composition of OA online (time resolution 20 s) and tracked its processing at a mountain site in southeastern China, using an Extractive ElectroSpray Ionization inlet coupled with a Time-of-Flight Mass Spectrometer (EESI-ToF-MS). We identified 2084 molecular formulas and compared OA composition from three sample types ~~with adjacent time (<2 h)~~: cloud droplets (CD), interstitial aerosol ~~particles~~ (INT), and cloud-free aerosol ~~particles~~ (CF) in representative cloud episodes. CHO class was the dominant constituent, followed by CHON class. ~~The~~In most cloud episodes, the fraction of CHO was lower in CD than that in INT and CF, while the fraction of CHON was higher, which may result from the uptake of organonitrates or nitration in cloud water. Compounds in CD had more carbon, ~~oxygen, and nitrogen~~ number but lower O/C and higher molecular weight than ~~INT and~~ CF, which is attributed to accretion reactions in cloud water. We identified ~~aqSOA tracers, including 39 new compounds, which were~~ significantly enriched compounds in CD compared with CF, which could be potentially used as aqSOA tracers formed via cloud processing. This study also reveals rapid changes ~~of~~in aqSOA composition, which highlight the necessity for high time resolution ~~measurement~~measurements to capture the processing of aqSOA in ~~clouds~~. Overall, this study provides clear information ~~of~~on processing of aqSOA in ~~clouds~~ and highlights the importance of accretion reactions, which ~~has~~have implications on the composition and physicochemical properties of SOA.

1 Introduction

40 Secondary organic aerosol (SOA) is a major component of organic aerosol (OA) with diverse emission sources, gaseous precursors, and composition, exerting significant impacts on air quality, climate, and human health (Jimenez et al., 2009; Nault et al., 2021). SOA is primarily produced through the oxidation of volatile organic compounds (VOCs), while the atmospheric aging of primary organic aerosol (POA) may also contribute. Numerous previous studies have investigated the formation mechanisms of SOA, with particular emphasis on gas-phase pathways (Odum et al., 1996; Ervens et al., 2011). However, SOA
45 formed solely through gas-phase reactions (gasSOA) cannot fully account for the observed SOA concentrations (de Gouw et al., 2005; Volkamer et al., 2007; Volkamer et al., 2006). In addition to the traditional gas-phase processing, aqueous-phase pathways have been recognized as an important source of SOA, ~~as supported by laboratory studies~~ (Ervens et al., 2011; Sehested et al., 1975; Galloway et al., 1976; Graedel and Weschler, 1981; Fu et al., 2008; Tan et al., 2009; Zhang et al., 2010; Ervens et al., 2011; Lamkaddam et al., 2021) ~~and model simulations~~ (Fu et al., 2008; Lamkaddam et al., 2021).

50 Mounting evidence for aqueous secondary organic aerosol (aqSOA) has been reported in field observations in various atmospheric aqueous systems, i.e., aerosol liquid water (ALW), fog water, and cloud water. For example, several studies on source apportionment in different sites showed that aqSOA formed in ALW is an important contributor to SOA, with its fraction particularly elevated (up to 44 %) under high relative humidity (RH) conditions ~~and during foggy or cloudy days~~ (Wang et al., 2021; Zhao et al., 2019; Tong et al., 2021; Gilardoni et al., 2016; Duan et al., 2022; Xu et al., 2019; Sun et al.,
55 2016). ~~In fog water, Duan et al. (2021) identified aqSOA and investigated the contribution and formation processes of aqSOA. Additionally, fog water samples were analyzed and compared with aerosol in OA composition (Brege et al., 2018; Kim et al., 2019; Gilardoni et al., 2016). Fog water and cloud water are both diluted aqueous systems. In contrast to fog, cloud is more common, ubiquitously presents in the atmosphere, and consists of a large quantity of droplets generated by aerosol activation, providing an aqueous medium for physical processes and chemical reactions (McNeill et al., 2012; McNeill, 2015). Cloud or~~
60 ~~fog processing affects OA in many aspects, including composition, concentration, size distribution, hygroscopicity, oxidation state, and can form brown carbon such as heterocyclic compounds, thus potentially affect air quality and radiation balance of the atmosphere (Wang et al., 2024; Chen et al., 2024; Jimenez et al., 2009; Altieri et al., 2008; Gramlich et al., 2023; Motos et al., 2019). Relative to ALW, fog water and cloud water are diluted aqueous systems where aqSOA can also be formed (Herckes et al., 2013). For fog water, the ratio of aqSOA to OA during fog-rain days is enhanced compared with non-fog-rain days~~
65 ~~(Duan et al., 2021). Additionally, OA composition of fog water is more oxidized (Brege et al., 2018), has more N-containing compounds (Mattsson et al., 2025; Sun et al., 2024a; Kim et al., 2019) compared with aerosol particles, and shows signs of oligomerization based on fragments in the mass spectrum (Gilardoni et al., 2016; Mandariya et al., 2019). In contrast to fog, the cloud is more common, ubiquitously presents in the atmosphere, and consists of a large quantity of droplets generated by~~

70 aerosol activation, providing an aqueous medium for physical processes and chemical reactions (McNeill et al., 2012; McNeill, 2015). Within clouds, aerosol particles may undergo repeated hydration-dehydration cycles, including hygroscopic growth, activation, and subsequent evaporation. Such cloud processing could influence the concentration of OA composition (Wang et al., 2024b; Gao et al., 2023; Liu et al., 2023b), thereby influencing aerosol size distribution, hygroscopicity, volatility, and cloud condensation nuclei (CCN) activity (Jimenez et al., 2009; Sun et al., 2025). Additionally, cloud processing may facilitate the formation of brown carbon, including N-containing heterocyclic compounds, which could affect atmospheric radiative forcing (Liu et al., 2023b).

75 ~~Many~~A number of field campaigns have been conducted to ~~investigate characteristics~~measure the chemical composition of ~~aqSOA~~OA in cloud droplets. Several previous field campaigns ~~investigated OA formation during cloud processing using~~ found that more highly oxygenated OA is present in cloud droplets compared to cloud-free aerosol ~~mass spectrometer particles~~ using online techniques, Aerosol Mass Spectrometer (AMS) or ~~aerodyne aerosol chemical speciation monitor~~Aerodyne
80 Aerosol Chemical Speciation Monitor (ACSM), which ~~obtained~~provide information on fragment ions of compounds, such as the fraction of m/z 44 (CO₂⁺) in the mass spectra (Dadashazar et al., 2022; ~~Gao et al., 2023~~; Lance et al., 2020; ~~Karlsson~~Gao et al., ~~2022~~2023). ~~Other~~Although these studies ~~applied single particle mass spectrometry (SPMS) to investigate the~~ composition of aqSOA in cloud droplets (Zhang et al., 2024a; Lin et al., 2017). However, studies using ~~provide valuable~~ information on the chemical composition of aqSOA, the use of AMS or ~~SPMS~~ACSM leads to molecular fragmentation and
85 ~~thus~~ cannot provide molecular ~~information on formulas for the components of aqSOA~~. As a result, the molecular composition of aqSOA, ~~hindering a detailed understanding of its chemical composition as well as the~~ and mechanisms of its formation and transformation ~~Although~~ remain incompletely understood. This gap hinders the analysis of sources, evolution, health effects, and climate impacts with respect to specific OA compounds.

90 Molecular formulas of OA in cloud samples can be assigned and classified into several groups, including CHO, CHON, CHOS, and CHONS, with CHO and CHON accounting for the largest fractions (Liu et al., 2023b; Cook et al., 2017; Pailler et al., 2024; Zhao et al., 2013; Bianco et al., 2019; Sun et al., 2021; Gramlich et al., 2023). Oligomers (Cook et al., 2017; Zhao et al., 2013), organosulfates (Sun et al., 2021; Bianco et al., 2019), and N-containing compounds such as nitroaromatics (Sun et al., 2021; Cook et al., 2017; Bianco et al., 2019) have been observed in cloud droplets. Although the molecular composition of OA in cloud droplets has been characterized using ~~offline analysis using instruments such as Gas Chromatography Mass~~
95 ~~Spectrometer (Collett et al., 2008), and~~ techniques such as Fourier Transform Ion Cyclotron Resonance Mass Spectrometry (FT-ICR-MS), the formation mechanisms of many compounds in clouds remain uncertain. For example, it is not clear whether the oligomers originate from cloud processing or from aqueous aerosol due to a lack of concomitant aerosol measurements and limited temporal variation analyses (Sun et al., 2021; Cook et al., 2017; Pailler et al., 2024; Liu et al., 2023b; Zhao et al.,

2013; Bianco et al., 2019) can provide molecular information, the time resolution of several hours or even one day limited by
100 offline filter sampling is insufficient to capture the variations of aqSOA in cloud. In a word, due to limited-. The coarse time
resolution of filter-based sampling (several hours to one day), together with limited sample numbers, prevents these studies
from resolving cloud-processing reaction processes that occur on minute-to-hour timescales and are subjected to the influence
of rapid variability in meteorological conditions within clouds. The chemical characteristics of aqSOA obtained from
comparisons between cloud droplets and cloud-free aerosol particles are subject to large uncertainties, because the composition
105 of both cloud droplets and aerosols may change over long-time and chemical resolution of previous measurements sampling.
Therefore, it is necessary to obtain online molecular information of aqSOA in cloud to provide on OA in clouds by comparing
OA composition of cloud droplets, interstitial aerosol particles, and cloud-free aerosol particles, to provide new insights into
the detailed chemical composition, evolution variation, and the mechanism of its chemical processes cloud processing.

To get a detailed understanding of cloud processing of aqSOA, we measured the real-time molecular composition of
110 aqSOA in ~~cloud~~clouds using an Extractive ElectroSpray Ionization inlet coupled with a Time-of-Flight Mass Spectrometer
(EESI-ToF-MS) in a mountain site in southeastern China. In this study, we identify molecular formulas of OA in cloud
processing and compare differences in OA characteristics between cloud droplets (CD), interstitial aerosol particles (INT), and
cloud-free aerosol particles (CF). We explore new compounds formed in cloud processing and explain their potential formation
mechanisms. We also aim to track the temporal evolution of compounds in aqSOA during cloud processing.

115 2 Methods

We conducted this field campaign from May 1st to May 29th in 2024 at Shanghuang Eco-Environmental Observatory of
Chinese Academy of Sciences at the summit of the Damaojian mountain (119.51° E and 28.58° N, 1128 m above sea level)
~~that is~~ located in Jinhua city, Zhejiang province, China. The site is a background monitoring station surrounded by coniferous
and broad-leaved forests away from megacities, as shown in Fig. 1. In addition to biogenic emissions, this site may be affected
120 by anthropogenic activities originating from the surrounding small counties, as mentioned in Zhang et al. (2024b2024).

Cloud droplets (CD) were collected using a Ground-based Counterflow Virtual Impactor (GCVI, Brechtel Manufacturing
Inc., Model 1205). The GCVI collected CD with diameters larger than 8.5 μm (Shingler et al., 2012) under conditions of
visibility < 3 km, RH > 95 %, and absence of precipitation. After separation from INT (non-activated aerosol in ~~cloud~~clouds),
the CD were dried by mild heating (40 °C) within the GCVI (Lin et al., 2017) and further by a Nafion dryer downstream, and
125 the residues of CD were subsequently measured. We note that the term “CD” in the Results and Discussion section refers to
the residues of cloud droplets. Because the focus is on the relative compositional change of OA in CD and CF, the GCVI
enhancement factor was not applied. A PM_{2.5} (particulate matter smaller than 2.5 μm) cyclone inlet (URG, USA) was used to

collect INT and CF. A switching system alternated between the GCVI and the URG inlet: PM_{2.5} was sampled when GCVI detected no cloud, whereas CD sampling was triggered automatically once cloud presence was detected by GCVI. During cloud episodes, the switch was also configured to alternate between CD and INT sampling. It should be noted that the terms “cloudy days” and “cloudless days” in this study specifically refer to periods with and without low clouds.

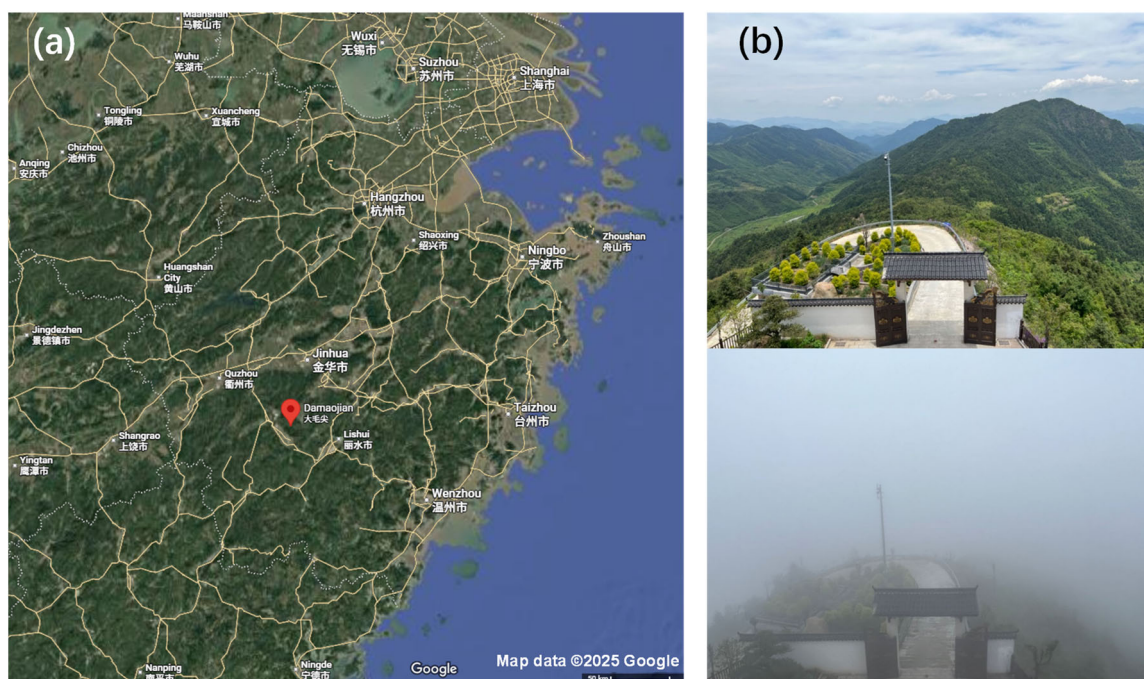


Figure 1. Location of the Shanghuang site. (a) a map (from Google Maps) and (b) two photos of [the](#) sampling site, one with cloud and another without cloud.

Measurements of CD, INT, and CF were conducted through a manifold positioned downstream of both the GCVI and URG inlets. The concentrations of OA composition were measured online using EESI-ToF-MS (Aerodyne Institute) with a time resolution of 20 s. This mass spectrometer achieves soft ionization while preserving the structure of compounds, measuring molecular formulas with high mass resolution (8000–10000) and low detection limit. [Detailed information regarding EESI ToF MS has been reported previously in Lopez-Hilfiker et al. \(2019\) and our previous studies \(Luo et al., 2024\) and \(Xue et al., 2025\). Here is a brief introduction. \(Wang et al., 2024a\). Detailed information regarding EESI-ToF-MS has been reported previously \(Lopez-Hilfiker et al., 2019; Stefenelli et al., 2019; Brown et al., 2021; Kumar et al., 2022; Luo et al., 2024; Xue et al., 2025\).](#) Aerosol was sampled after gaseous compounds were removed by entering a charcoal denuder, and subsequently intersected with an electrospray generated from a working solution containing 100 ppm NaI in a 1:1 (v/v) water and acetonitrile mixture, allowing aerosol compounds to be detected as $[M+Na^+]\text{I}^+$ in positive ion mode. Background measurements were obtained by switching the inlet to a filter. The durations of sample and background collection can be adjusted to ensure aerosol signal levels return to baseline within the time of background (Qi et al., 2019). In this campaign, [the](#) sample and background were set in combinations of 10 min and 5 min typically. The sampling volume of EESI-ToF-MS was 0.9 L m⁻³. Weekly calibration was performed using levoglucosan, and the sensitivity was assumed identical for all compounds.

~~This assumption does not affect our results since we specifically focus on relative compositional changes of OA in CD and CF as mentioned above.~~ All organic compound signals are shown as relative intensities normalized to (NaI)Na⁺ to avoid interference from the ion source fluctuations in EESI-ToF-MS. Mass spectral data were processed using Tofware 3.2.5 in Igor Pro 8. For data screening, the signal-to-background ratio (s/b) was calculated as the median value of (sample signal-background)/background, thereby excluding compounds showing insignificant differences between sample and background. Only compounds with the s/b ratio greater than 0.1 were included (Tong et al., 2021). After this screening, 79, 148, 604, and 126 compounds were retained from cloud episodes one to four, respectively. All results presented in Sect. 3.2 are based on these screened data.

The OA size distribution was characterized using a scanning mobility particle sizer (SMPS, TSI 3936), which, together with an atomizer (TSI, 3076), was used to facilitate EESI-ToF-MS calibration. PM_{2.5} concentration was monitored using a Thermo Scientific instrument (Thermo Scientific. Model 5014i), while CO was measured by a Picarro greenhouse gas analyzer (Picarro Inc., G2401). Meteorological parameters including RH, Temperature (T), wind speed (WS), and wind direction (WD) were monitored by an automatic weather station.

The 72 h backward trajectories of air masses arriving at the Shanghuang site were calculated by [the](#) Hybrid Single-Particle Lagrangian Integrated Trajectory (HYSPLIT) model, with Global Data Assimilation System (GDAS) meteorological data at 1°×1° spatial resolution (Stein et al., 2015; Rolph et al., 2017). These trajectories were clustered into several appropriate groups for ~~4 CEs~~ [selected cloud episodes](#). The clustering was based on the total spatial variance (TSV) method (Song et al., 2023; Roland et al., 2025).

3 Results and discussion

3.1 Characteristics of cloud episodes

During the entire campaign, PM_{2.5} concentration was 13.4±10.8 μg m⁻³ (mean value ± standard deviation), with the highest concentration of 72.2 μg m⁻³ observed on cloudless days, as shown in Fig. 2. The PM_{2.5} concentration is typical in rural areas of China and is substantially lower than that observed in the same season in metropolitan cities such as Beijing (~40 μg m⁻³) and Shanghai (~30 μg m⁻³) (Liu et al., 2023a; Yin et al., 2023).

Cloud episodes accounted for 27.1 % of the one-month campaign, with the sample types of CD and INT representing 13.1 % and 14.0 %, respectively. Of the 16 recorded cloud episodes, we selected those without precipitation and with adjacent cloud-free periods (<2 h from CD) to avoid the influence of wet deposition and ensure CD/INT/CF sampling coverage. Six out of 16 episodes meet these criteria, and four cloud episodes (CEs) are further selected. CE1, CE2, CE3, and CE4 differ in PM_{2.5} and CO concentration, meteorological conditions, origin of air mass, and duration time, as shown in Table S1. The

duration of each CE ranged from several minutes to three days. Meteorological conditions and origin of air masses are discussed in Text S1, and backward trajectories from HYSPLIT are shown in Fig. S2.

180

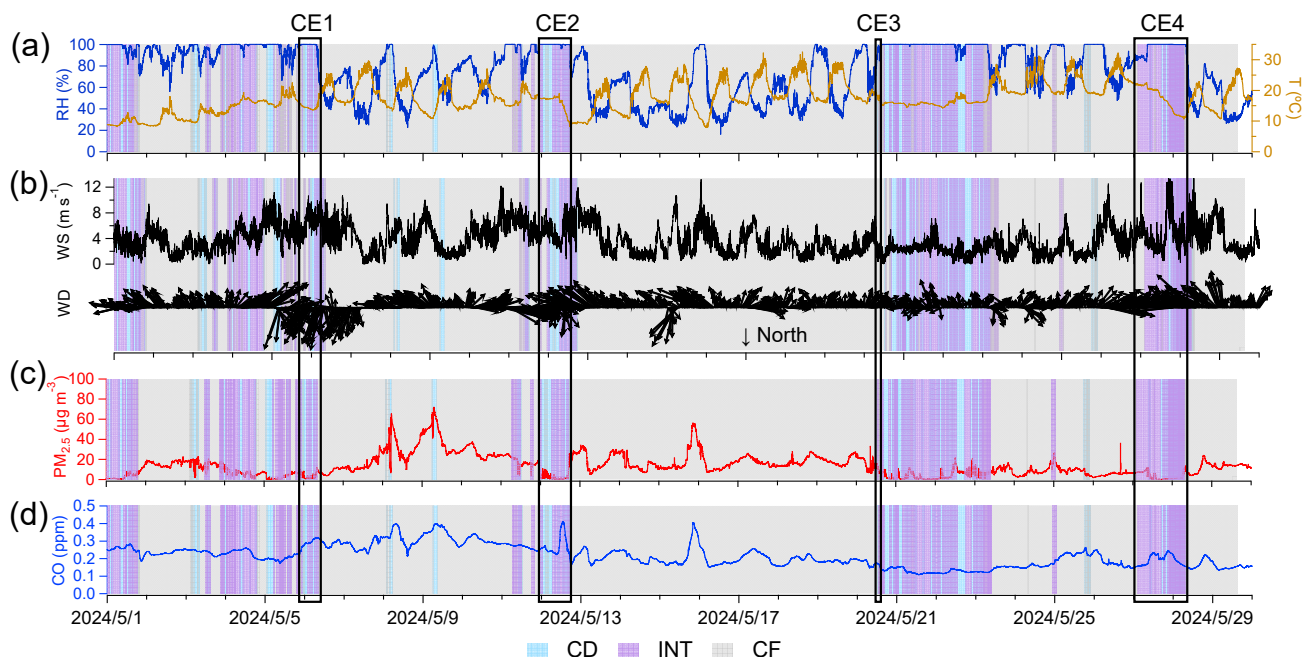


Figure 2. Time series of (a) RH and T, (b) WS and WD, (c) PM_{2.5}, and (d) CO. Sample types of cloud droplets (CD), interstitial aerosol particles (INT), and cloud-free aerosol particles (CF) are shaded as blue, purple, and gray, respectively.

Each CE's sampling period is divided into three stages (pre-cloud, in-cloud, and post-cloud) to compare OA characteristics. The in-cloud stage corresponds to the sample types of CD and INT, whereas both the pre-cloud and post-cloud stages correspond to the sample type of CF (PM_{2.5}). Detailed characteristics of sample types in four CEs, such as mean chemical formula, H/C, O/C, N/C, and OSc (carbon oxidation states, 2×O/C–H/C), are shown in Table 1, and division of stages is shown in Fig. S1.

A total of 2084 molecular formulas of OA were identified in the campaign. Mean formula of CD was $C_{40.04}H_{14.59-20.34}O_{5.08-9.2}N_{0.34-0.32}S_{0.42}Si_{0-0.01}$ for CE1–CE4. Compared with pre-cloud aerosols with formula $C_{8.43-11.10}H_{14.23-17-10.57}O_{5.06-14}N_{0.12-0.35}S_{0.30}Si_{0-0.28}$, CD exhibited increased numbers of carbon, hydrogen, oxygen, and nitrogen atoms, with the differences being statistically significant ($p < 0.05$) (Table S2). These molecular formulas were classified into eight classes, that is, CHO (only C, H, O atoms are contained in the chemical formula, hereafter), CHON, CHONS, CHOS, CHN, CHS, CHNS, and CHOSi. Since the composition of OA varied in different CEs, the fractions of these OA classes are discussed for each CE in Sect. 3.2. The O/C ratio was generally lower in CD (0.45–0.66) than in pre-cloud aerosols, INT, and post-cloud aerosols in 4 CEs. The O/C ratio in CD is comparable to those reported for fog water (0.52–0.68), aqSOA (0.61–0.84), and oxygenated OA (0.44–0.83) by Gilardoni et al. (2016). In general, O/C of CD in this study is comparable to that of fog (0.58–0.8) in the Po Valley in Brege et al. (2018), while H/C of CD (1.4950–1.8287) is

190

195

lower/higher than that of fog (1.29–1.37) in that study. Furthermore, CD showed elevated N/C (0.034033–0.047045) relative to other sample types, while its OSc value (–0.7283 to –0.2425) is generally lower than in other sample types.

Table 1. Detailed characteristics Mean molecular formulas and elemental parameters (H/C, O/C, N/C, and OSc; mean ± standard deviation) of OA chemical composition for CE1–CE4 in pre-cloud aerosols, CD, INT, and post-cloud aerosols. Shown are the mean chemical formulas and the mean H/C, O/C, N/C, and OSc values.

	Pre-cloud aerosols	CD	INT	Post-cloud aerosols
CE1 Formula	$C_{9.10}H_{14.27}O_{5.72}N_{0.24}S_{0.28}Si_{0.28}C_8$	$C_{10.45}H_{16.69}O_{6.00}N_{0.34}S_{0.55}Si_{0.55}H$	$C_{9.20}H_{14.41}O_{5.72}N_{0.27}S_{0.24}C_8$	$C_{9.28}H_{14.73}O_{5.79}N_{0.26}S_{0.36}C_{8.86}$
H/C	1.6061±0.04	1.6064±0.11	1.5961±0.04	1.5961±0.04
O/C	0.7071±0.02	0.66±0.03	0.69±0.02	0.6970±0.02
N/C	0.025022±0.004	0.034033±0.008	0.028±0.005	0.028025±0.006
OSc	–0.2419±0.06	–0.2933±0.14	–0.2422±0.06	–0.20±0.06
CE2 Formula	$C_{8.62}H_{14.23}O_{5.06}N_{0.31}S_{0.33}H_{13.72}$	$C_{10.45}H_{18.84}O_{5.45}N_{0.41}S_{0.13}H_{19.51}$	$C_{8.79}H_{14.56}O_{5.00}N_{0.35}S_{0.52}H_{14.19}O$	$C_{11.04}H_{19.73}O_{6.14}N_{0.38}S_{0.12}H_{21.10}$
H/C	1.6970±0.03	1.8287±0.15	1.7072±0.04	1.7478±0.13
O/C	0.63±0.01	0.58±0.03	0.61±0.02	0.6061±0.02
N/C	0.038037±0.004	0.047045±0.01	0.043042±0.009	0.037031±0.006
OSc	–0.4443±0.04	–0.6671±0.19	–0.4950±0.08	–0.5056±0.15
CE3 Formula	$C_{11.10}H_{16.83}O_{5.07}N_{0.35}S_{0.10}Si_{0.57}H$	$C_{12.81}H_{20.34}O_{5.08}N_{0.43}S_{0.92}H_{21.78}$	$C_{10.88}H_{16.77}O_{5.07}N_{0.31}S_{0.005}Si_{0.10}$	$C_{11.06}H_{16.84}O_{5.09}N_{0.32}S_{0.10}Si_{0.51}H_1$
H/C	1.5657±0.01	1.6373±0.08	1.5859±0.01	1.5658±0.01
O/C	0.5355±0.008	0.45±0.03	0.5355±0.005	0.5355±0.005
N/C	0.036033±0.002	0.044040±0.007	0.034028±0.002	0.033029±0.002
OSc	–0.5448±0.02	–0.7283±0.12	–0.5249±0.02	–0.5047±0.02
CE4 Formula	$C_{8.43}H_{13.27}O_{5.36}N_{0.16}S_{0.17}H_{12.99}$	$C_{10.01}H_{14.59}O_{5.72}N_{0.34}S_{0.95}H_{14}$	$C_{9.13}H_{13.56}O_{5.56}N_{0.23}S_{0.003}Si_{0.89}$	$C_{8.94}H_{13.36}O_{5.57}N_{0.20}S_{0.003}Si_{0.87}$
H/C	1.6465±0.02	1.4950±0.04	1.5452±0.02	1.52±0.01
O/C	0.6869±0.01	0.62±0.02	0.6566±0.008	0.67±0.01
N/C	0.018014±0.005	0.034±0.01	0.024021±0.005	0.022019±0.003
OSc	–0.28±0.04	–0.2425±0.07	–0.20±0.02	–0.18±0.02

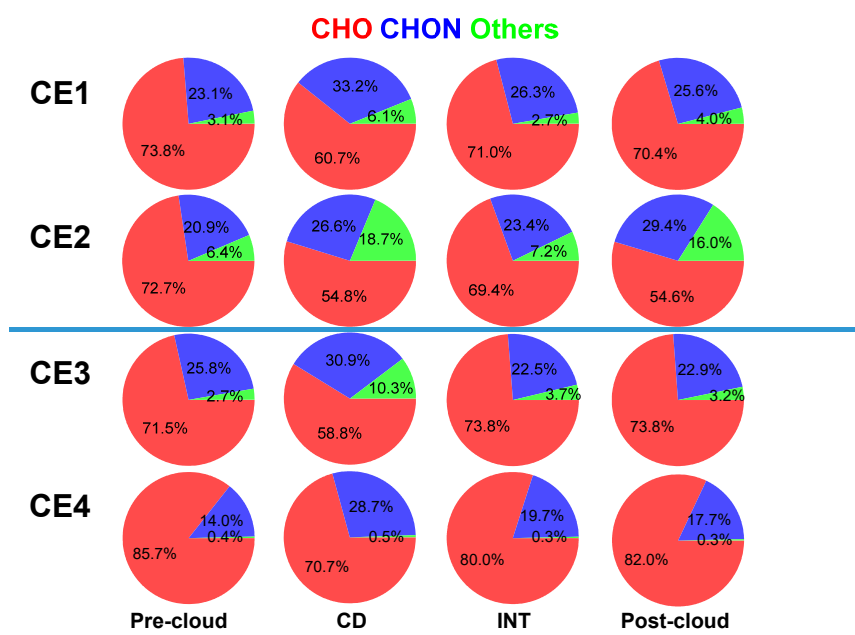
205

3.2 Comparison of cloud episodes

The fractions of three OA classes which are CHO, CHON, and Others (including CHONS, CHOS, CHN, CHS, CHNS, and CHOSi) exhibited general similarities across the four CEs, as shown in Fig. 3. In all sample types (pre-cloud aerosols, CD, INT, and post-cloud aerosols) of the four CEs, CHO dominated OA composition, accounting for > 50 % of signal intensity of OA (54.6 %–85.7 % from CE1 to CE4), followed by CHON (14.0 %–33.2 %) and Others (lower than 18.7 %). The Others class, predominantly CHOSi, accounted for 0.5 %–18.7 % in CD, exceeding the fractions in other sample types, and is further discussed at the level of individual compounds below. Generally in most cloud episodes, CD showed the lowest CHO fraction (54.8 %–70.7 %) and the highest CHON fraction (26.6 %–33.2 %) among the four sample types. The only exception is in CE2, with the higher CHON (29.4 %) and lower CHO (54.6 %) in post-cloud aerosols than in other sample types, is attributable to air mass changes during the long-time interval between post-cloud and others (shown in Fig. 2 and Fig. S1), as indicated

215

by elevated CO concentration. CHON compounds have been detected in cloud and fog water in numerous studies (LeClair et al., 2012; Sun et al., 2024a; Sun et al., 2021; Sun et al., 2024b). Higher CHON fraction (59.0 %–63.5 %) in fog water than aerosol particles (51.2 %–51.5 %) was reported previously in Sun et al. (2024a), which is in agreement with the results in this study. In addition, the greater number of CHON compounds in CD compared with CF underscores the role of cloud processing in enhancing CHON, as reflected in [the](#) number fraction rather than [the](#) intensity fraction (Boone et al., 2015; Liu et al., 2023b). The fraction of CHON (19.7 %–26.3 %) in INT was lower than in CD (26.6 %–33.2 %) and higher than in pre-cloud aerosols (14.0 %–23.1 %) in CE1, CE2, and CE4. However, in CE3, the slightly lower CHON fraction in INT compared to pre-cloud aerosols may be due to [fluctuation/turbulence](#) in [cloud/clouds](#) resulting from the short duration time of the cloud (several minutes). Higher relative abundance of CHON in CD (43.6 %–65.3 %) compared to INT (31.8 %–51.0 %) has been observed at Tianjing Mountain in southern China (Sun et al., 2021), consistent with our results. The higher CHON fraction in CD than in pre-cloud aerosols suggests that cloud processing promoted CHON formation. Higher CHON in INT compared to pre-cloud aerosols indicates that although not activated into cloud droplets, high RH experienced by INT (close to 100 %) and corresponding high aerosol water content could still promote CHON formation in INT, consistent with the elevated N/C ratio of aqSOA of aerosol particles under high RH conditions (Zhao et al., 2019). [We would like to note that it is assumed that different classes of compounds have similar sensitivity in EESI-ToF-MS.](#)



~~Figure 3. Fractions of three classes of OA, namely CHO, CHON, and Others (including CHONS, CHOS, CHN, CHS, CHNS, and CHOS) in pre-cloud aerosols, CD, INT, and post cloud aerosols in CE1, CE2, CE3, and CE4.~~

Among the CHON class, the compounds enriched in CD, such as $C_{8-12}H_{11-19}NO_{5-8}$ and $C_{14-16}H_{21-27}NO_{4-9}$, with an O/N ratio of ≥ 3 (69.71 %–88 % for CE1–4, CE3, and CE4, and 17% for CE2), suggesting that they are likely organonitrates, amino acids, or [nitrogen-N-containing](#) heterocyclic compounds. At the Shanghuang site, emissions of monoterpenes and sesquiterpenes are abundant (Zhang et al., 2024b, 2024). Consequently, $C_{10}H_{15}NO_x$ and $C_{10}H_{17}NO_x$ may be formed via hydroxyl

oxidation of monoterpene in the presence of NO (Shen et al., 2022) or NO₃ oxidation (Shen et al., 2021; Guo et al., 2022) and dissolve in the aqueous phase, whereas C₁₅H₂₃NO_x and C₁₅H₂₅NO_x may originate from similar reactions involving sesquiterpenes. Additionally, precursors could form organonitrates through aqueous reactions, e.g., with NO₃ radicals (Ng et al., 2017), or involving NO₃⁻ (Sun et al., 2024b; Huang et al., 2023; Barber et al., 2024). These reactions can occur at night or even during the day under reduced light conditions in ~~cloud~~clouds. This finding contrasts with the observation at Mt. Tai, where, despite the higher number of CHON compounds in CD relative to CF, a larger fraction contained reduced nitrogen groups (O/N <3) (Liu et al., 2023b). Such disparity may arise from differences in precursors between the two sampling sites. Additional information, such as the gas-phase CHON composition and concentration, is required to further elucidate the formation mechanisms of these compounds.

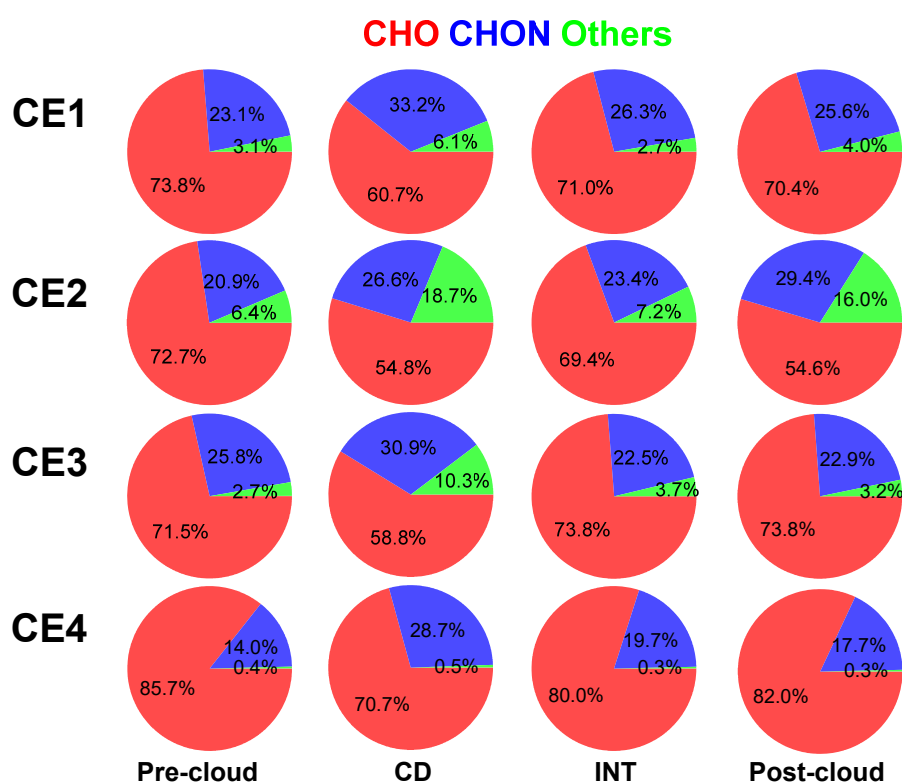
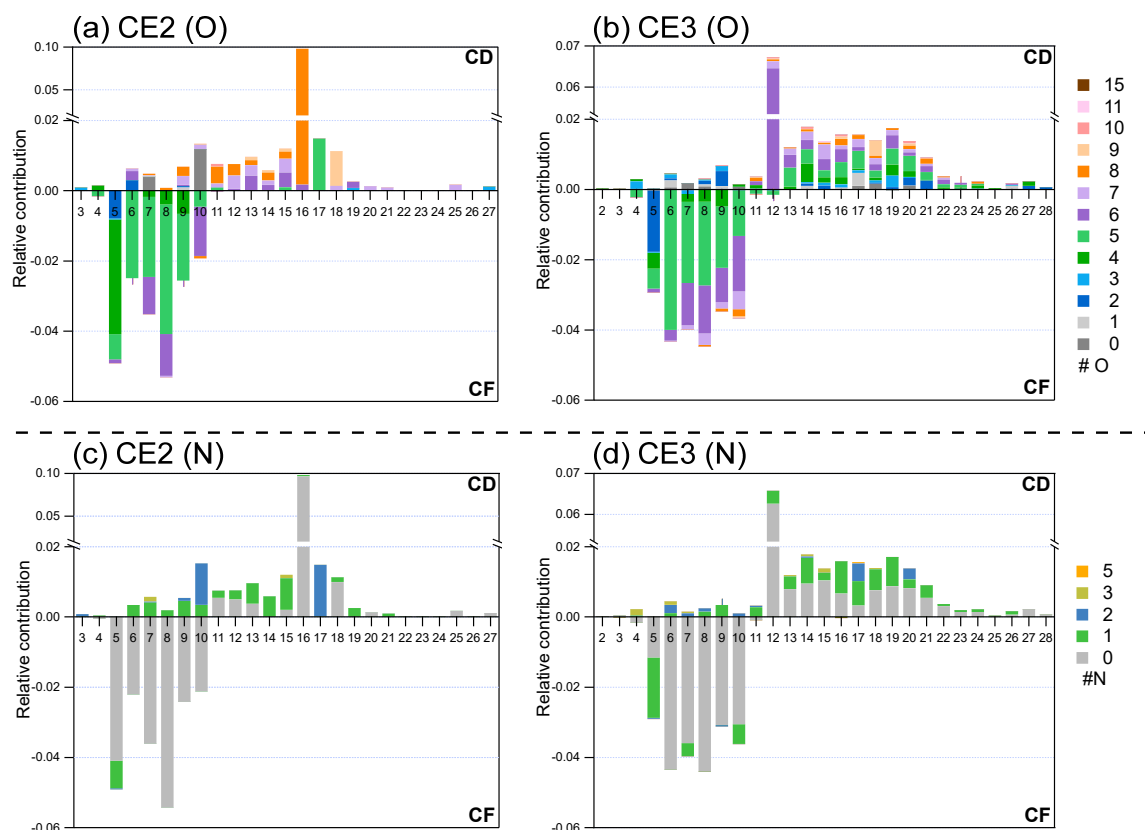


Figure 3. Fractions of three classes of OA, namely CHO, CHON, and Others (including CHONS, CHOS, CHN, CHS, CHNS, and CHOSi) in pre-cloud aerosols, CD, INT, and post-cloud aerosols in CE1, CE2, CE3, and CE4.

The molecular composition characteristics of OA in four CEs exhibit similar patterns, presented as carbon number distribution colored according to the numbers of oxygen and nitrogen; therefore, only CE2 and CE3 are shown in Fig. 4 (CE1 and CE4 in Fig. S3). In each CE, comparison is carried out between CD and CF which was the closest to CD temporally: for CE1–3, CD is compared with pre-cloud aerosols, while CE4 is compared with post-cloud aerosols, as shown in Fig. S1. In CD, the carbon number of OA ranged from 2 to 28 (CE2: 3–27; CE3: 2–28), and the oxygen number ranged from 0 to 10 in CE2

and 0 to 15 in CE3. Comparing with OA in CF, OA in CD contained [a](#) higher fraction of compounds with $n_C > 10$ as well as elevated n_O (CE2: $n_O=7-10$; CE3: $n_O=6-15$).



260 **Figure 4. Detailed relative contribution of OA. The average carbon number distribution of differences between CD and CF are colored by oxygen number of (a) CE2, (b) CE3; and nitrogen number of (c) CE2, (d) CE3. Positive value stands for significant molecular characteristics of CD, and negative value stands for that of CF. Fractions of compounds are normalized to sum of signals of all organics in CD and CF, respectively.**

The nitrogen number (n_N) distributions relative to n_C exhibit similar patterns in all CEs. In CE2, the n_N of N-containing OA is distributed from 0 to 3, and from 0 to 5 in CE3. The n_C of N-containing OA ranged from 3 to 21 in CE2 and 4 to 27 in
 265 CE3. Compared with CF, CD contained a larger fraction of N-containing OA, especially those with $n_N=1-3$ and higher n_C . Collectively, compounds in CD had more n_C , n_O , and n_N than those in CF. [These molecular characteristics are likely attributed to accretion reactions such as oligomerization \(Yu et al., 2016\).](#) [The molecular characteristic of higher \$n_C\$ is likely attributed to accretion reactions such as oligomerization \(Yu et al., 2016; Fenselau et al., 2025\).](#) This finding is consistent with several laboratory studies of aqSOA formation. For instance, enriched high-molecular-weight compounds ([HMWC](#)) in aqSOA were
 270 reported in the bulk phase experiments of methylglyoxal and glyoxal under cloud-relevant conditions (Tan et al., 2009; Altieri et al., 2008). And aqSOA from in-cloud simulation using a wetted-wall flow reactor has more highly oxygenated and carbon-containing compounds than gasSOA simulated by an oxidation flow reactor (OFR) from the same biomass burning samples ([Wang et al., 2024](#)). ([Wang et al., 2024b](#)). Experiments in the bulk phase and the wetted-wall flow reactor which better

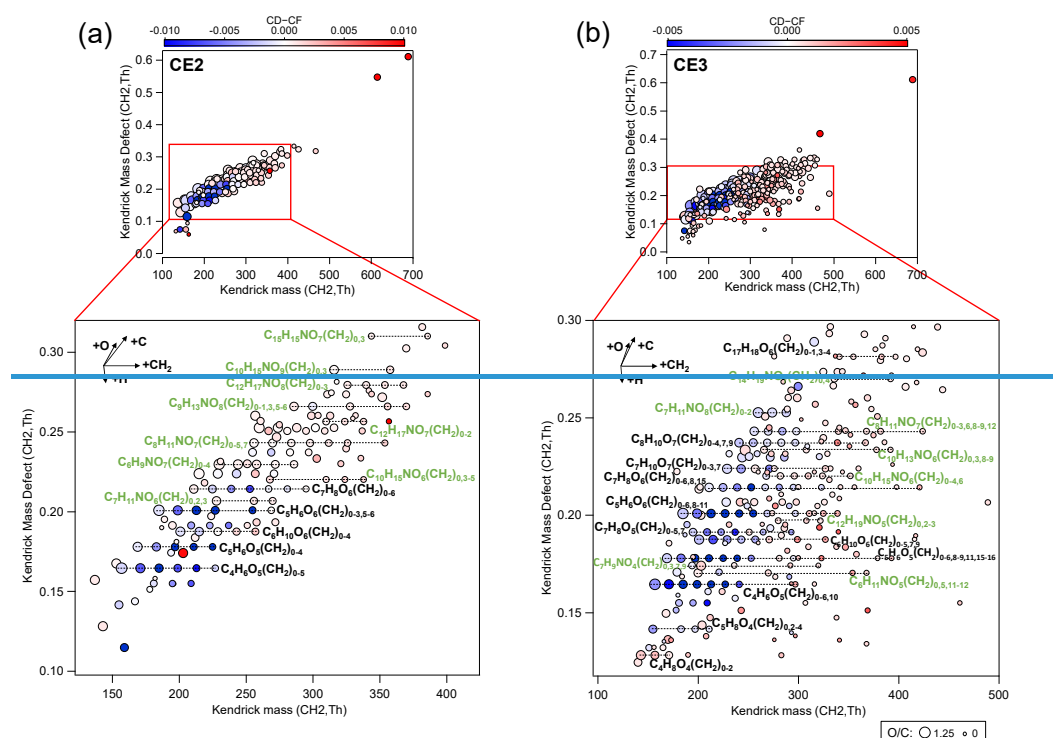
275 represents atmospheric aqueous conditions, indicate that accretion reactions could be prevalent in cloud droplets. [Field observations in the Arctic also show potential evidence of accretion reactions, with compounds of longer carbon chains enriched in CD relative to CF \(Pasquier et al., 2022\), hinting at the possible importance of accretion reactions. Notably, this study provides direct molecular-level evidence for the contribution of accretion reactions during cloud processing of OA.](#)

To investigate OA processing when the cloud episode changed from CF to CD, CH₂-based Kendrick mass defect (KMD) plots for CE2 and CE3 are analyzed (Fig. 5). The chemical formulas of compounds with a larger fraction in CD than CF in 280 four CEs are listed in Table [S2S3](#). Several series of compounds in CE2 and CE3 exhibit sequential increase in CH₂ groups, such as C₁₀H₁₅NO₆(CH₂)_n, C₈H₁₁NO₇(CH₂)_n, C₄H₆O₅(CH₂)_n, C₅H₆O₅(CH₂)_n, C₅H₆O₆(CH₂)_n, C₇H₈O₆(CH₂)_n. Specifically, numerous CHON compounds were present at higher fractions in CD, with some labeled by formulas such as series of C₆H₉NO₇(CH₂)₀₋₄, C₇H₁₁NO₆(CH₂)_{0,2,3}, C₈H₁₁NO₇(CH₂)_{0-5,7}, and C₁₂H₁₇NO₈(CH₂)₀₋₃ in CE2 and series of C₇H₉NO₄(CH₂)_{0,3,7,9}, C₈H₁₁NO₇(CH₂)_{0-3,6,8-9,12}, C₁₀H₁₅NO₆(CH₂)_{0-4,6}, C₁₂H₁₉NO₅(CH₂)_{0,2-3} in CE3. This result is in agreement with the higher 285 fraction of total CHON compounds in CD compared with CF, as discussed above. [The observed CH₂-based homologous series likely reflects carbon-chain growth through aqueous accretion reactions. Possible formation pathways include peroxy radical \(RO₂\) addition, aldol condensation, hydroxyl-carbonyl addition \(hemiacetal/acetal formation\), and esterification involving precursors \(Tilgner et al., 2021; Mayhew et al., 2025\), which warrant further investigation.](#) For most homologues, CD contained higher fractions of larger compounds (with more CH₂ groups) than CF, while lower fractions of smaller compounds. 290 As detailed above, it is likely that cloud processing enhanced accretion reactions by extending the length of the carbon chain, which further highlights the importance of accretion reactions of organics in cloud droplets. In CF, CHO had a larger fraction than CHON; for example, CHO compounds such as C₅H₆O₆(CH₂)_n, C₆H₁₀O₆(CH₂)_n, and C₅H₆O₅(CH₂)_n were more abundant. The pattern of adding CH₂ groups in cloud processing is similar in all CEs. However, the KMD ~~plot~~plots based on O ~~show~~show that compounds in CE2 and CE3 did not exhibit a clear pattern with a sequential increase in O (Fig. S4). The 295 dominant pattern of CH₂ addition, rather than O addition, suggests that sequential OH addition or auto-oxidation was not prevalent in cloud processing. In terms of the increments of CH₂ and O, CH₂ displays a wider growth trend (0–7) among all series, whereas O shows a narrower increase, confined to a range of 0 to 3. Consequently, results of KMD plots suggest that as cloud processing proceeded, n_C of OA increases, while the increase in n_O is lower than the n_C, agreeing with the lower O/C ratio in CD than that in CF. The possible reason is that aqueous processing is more significant in accretion (enhancing n_C) than 300 oxygenation (enhancing n_O).

[Some siloxane compounds showed higher fractions in CD than in CF, such as C₁₆H₄₈O₈Si₈ \(m/z 615\) and C₁₈H₅₄O₉Si₉ \(m/z 689\) in CE2 and C₁₂H₃₆O₆Si₆ \(m/z 467\) and C₁₈H₅₄O₉Si₉ in CE3. Siloxane is a type of volatile chemical products such as](#)

those found in personal care products (Gkatzelis et al., 2021; McDonald et al., 2018). To our best knowledge, this is the first time that $C_{16}H_{48}O_3Si_3$ was observed in cloud droplets. The reason for the higher fraction of siloxane warrants further study.

305



Furthermore, although oligomer formation involving subunits such as $C_2H_2O_3$ (Lim et al., 2010) and $C_3H_4O_2$ (Cook et al., 2017; Altieri et al., 2008; Tan et al., 2009) has been reported, compounds in CE of this study such as CE2 and CE3 did not seem to show clear sequential increases in these subunits (Fig. S5). This may be attributed to differences in precursors and formation mechanisms during cloud processing between the Shanghuang site and other observations and laboratory studies. In addition, some siloxane compounds showed higher fractions in CD than in CF. The reason for the higher fraction of siloxane warrants further study.

310

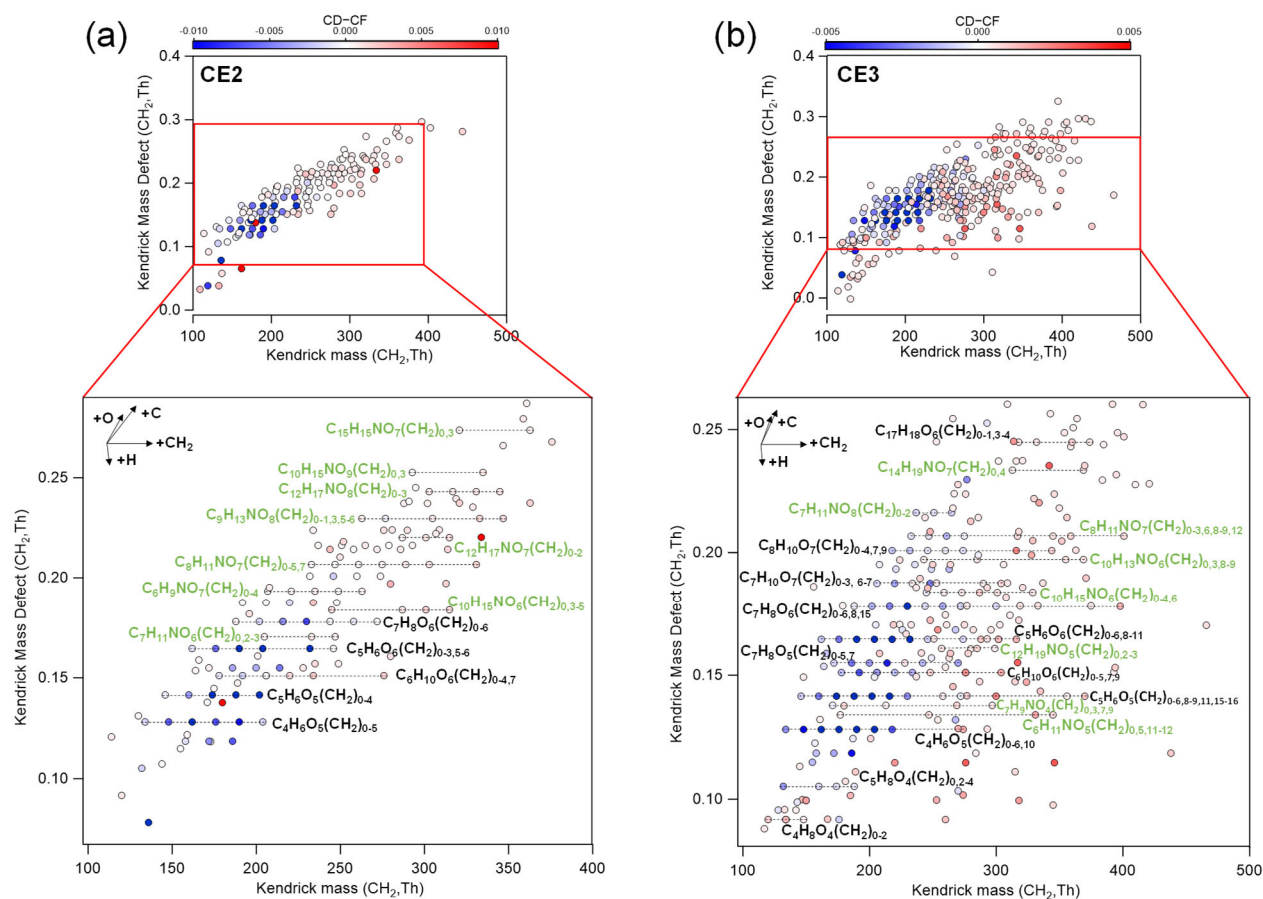


Figure 5. Kendrick mass defect m/z plots based on CH_2 of compounds in (a) CE2 and (b) CE3. Data points are color-coded by differences in fractions of compounds between CD and CF and sized by the O/C ratio. Fractions of compounds are normalized to the sum of signals of all organics in CD and CF, respectively. Note that, for conciseness, data points in CE3 with normalized signal difference between -0.0003 and 0.0003 (appearing nearly white) are not shown here. The molecular formulas include the reagent ion Na^+ , which is not shown here for simplicity and clarity.

3.3 Characteristic compounds in cloud processing and formation mechanisms

We identified aqSOA tracers in cloud droplets by comparing the intensity fractions of all compounds between CD and CF using a t -test at a significant level of 0.05. A total of 144, 421, 274, and 537 organic compounds in CE1, CE2, CE3, and CE4, respectively, passed the t -test. Among these compounds, 39 organic compounds in CD were significantly enriched in three or four CEs, as shown in Table 2. Two were consistently significant in CD across all four CEs: $\text{C}_{14}\text{H}_{42}\text{O}_7\text{Si}_7$ and $\text{C}_9\text{H}_{22}\text{N}_2\text{O}_4$. Furthermore, sulfate compounds were enriched in CD compared with CF in three CEs, of which time series is shown in Fig. S6. Sulfate is a well-established tracer for aqueous-phase processing, and its elevated concentration in cloud droplets and fog has been widely reported (Dadashazar et al., 2022; Brege et al., 2018; Kim et al., 2019). This result, which further confirms and enhances the reliability of identifying the identification of aqSOA tracers. Accordingly, these 39 enriched OA compounds can be regarded as aqSOA tracers formed via cloud processing. The number of CHO, CHON, CHN, and CHOSi compounds is 15, 19, 2, and 3, respectively. The majority of the enriched OA compounds exhibit

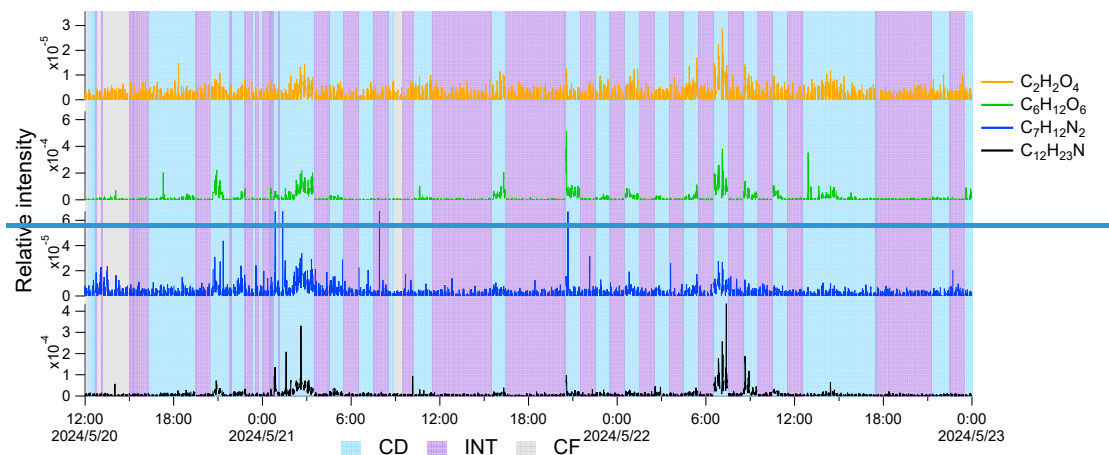
carbon numbers greater than nine, which is also an indication of accretion reactions in cloud droplets. Most of these [aqSOA tracers](#) enriched OA compounds have not been reported in previous literature (Cook et al., 2017; Bianco et al., 2019; Tong et al., 2021; Sun et al., 2024b).

335 **Table 2. Thirty-nine [aqSOA tracers](#) enriched OA compounds observed in CD of three or four CEs. These [tracers](#) OA compounds are classified into four classes: CHO, CHON, CHN, and CHOSi.**

CHO	CHON	CHN	CHOSi
C ₆ H ₁₂ O ₆	C ₄ H ₇ NO ₄	C ₉ H ₁₈ N ₂	C ₁₂ H ₃₆ O ₆ Si ₆
C ₁₀ H ₁₆ O ₂	C ₅ H ₁₁ N ₂ O	C ₁₂ H ₂₃ N	C ₁₄ H ₄₂ O ₇ Si ₇
C ₁₀ H ₂₂ O ₄	C ₉ H ₂₂ N ₂ O ₄		C ₁₆ H ₄₈ O ₈ Si ₈
C ₁₂ H ₂₆ O ₅	C ₉ H ₁₃ NO ₂		
C ₁₃ H ₂₂ O	C ₁₀ H ₁₉ NO		
C ₁₃ H ₂₆ O ₅	C ₁₀ H ₁₉ NO ₃		
C ₁₅ H ₂₄ O ₁₄	C ₁₁ H ₁₉ NO ₄		
C ₁₅ H ₂₆ O ₈	C ₁₃ H ₃₀ N ₂ O ₄		
C ₁₅ H ₃₂ O ₆	C ₁₃ H ₂₃ NO ₃		
C ₁₆ H ₃₀ O ₄	C ₁₄ H ₂₉ N ₃ O ₃		
C ₂₀ H ₂₂ O ₅	C ₁₄ H ₂₉ NO ₄		
C ₂₁ H ₃₆ O ₈	C ₁₈ H ₃₃ NO ₅		
C ₂₃ H ₄₄ O ₃	C ₁₈ H ₂₉ NO ₅		
C ₂₄ H ₄₀ O ₃	C ₁₉ H ₃₇ NO ₃		
C ₃₀ H ₅₆ O ₂	C ₂₀ H ₂₉ NO ₅		
	C ₂₁ H ₄₁ NO ₂		
	C ₂₂ H ₃₄ N ₂ O ₆		
	C ₂₉ H ₅₁ NO ₂		
	C ₂₉ H ₅₁ NO ₆		

Furthermore, 236 OA compounds were significantly enriched in two of four CEs, including the common aqSOA tracer, oxalic acid (C₂H₂O₄), previously reported in field observations and laboratory studies (Rogers et al., 2025; Ervens et al., 2011).

340 The compound C₂O₄Na₃⁺ is identified as oxalic acid, of which the hydrogen atoms in the carboxylic functional group (-COOH) are substituted by Na⁺ (Surdu et al., 2024). The oxalic acid signal was exclusively observed during CD, whereas it remained weak and noisy in CF and INT, as shown in Fig. 6. ~~Overall, the~~The oxalic acid signal was ~~not significant~~ significantly enhanced only in CE2 and CE4, rather than in all four CEs, ~~primarily attributed~~ which may be related to ~~large fluctuations~~ larger inhomogeneity within clouds due to strong turbulence. Meanwhile, the C₆H₁₂O₆ signal was as low as the detection limit in CF; 345 however, it increased gradually when CD began. C₆H₁₂O₆ in aqueous formation was reported in a laboratory study and may be produced from the aqueous reaction of formaldehyde or acetaldehyde (Li et al., 2011). Therefore, it is reasonable to classify C₆H₁₂O₆ as a tracer of aqSOA.



Notably, N-

350

containing compounds were significant in CD, such as $C_{12}H_{23}N$ and $C_7H_{12}N_2$ (shown in Fig. 6). $C_{12}H_{23}N$ was reported to be emitted from primary sources including vehicle emissions (Thomas et al., 2025) and agricultural residue burning (Lin et al., 2012), whereas $C_7H_{12}N_2$ (enriched in CE2) has been observed in emissions from traditional biomass fuel burning and agricultural residue burning (Fleming et al., 2018; Wang et al., 2017; Lin et al., 2012; Hao et al., 2025). $C_{12}H_{23}N$ and $C_7H_{12}N_2$ may be formed in aerosol phase and undergo uptake into cloud droplets. These compounds could also be heterocyclic compounds containing imine or amine functional groups, potentially resulting from secondary formation in the aqueous phase (Zhao et al., 2015; Li et al., 2023). In addition, $C_{12}H_{23}N$ may be a compound with a pyrrole structure.

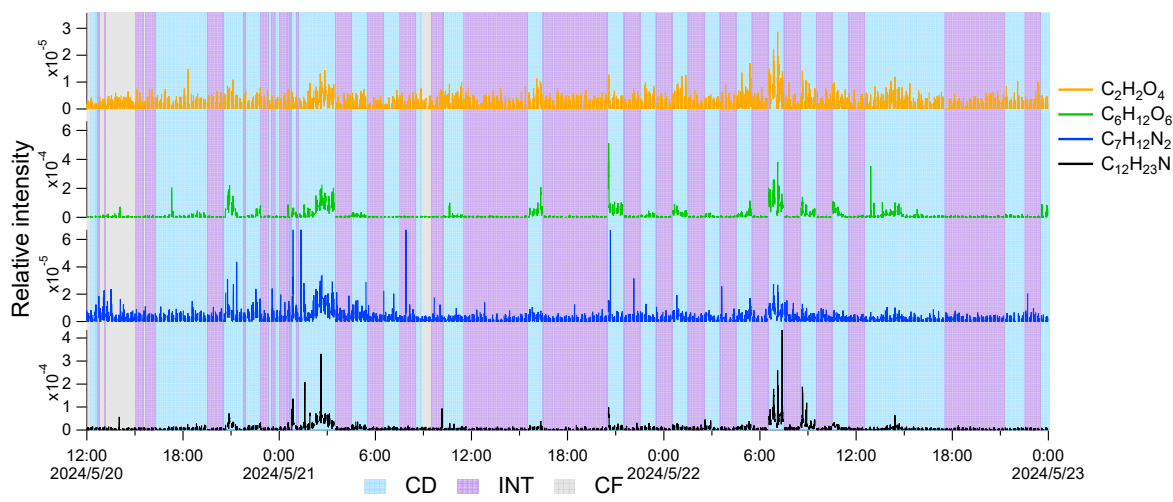
355

~~Figure 6. Time series of compounds: carboxylic acid ($C_2H_2O_4$), $C_6H_{12}O_6$, nitrogen-containing substances including $C_7H_{12}N_2$ and $C_{12}H_{23}N$, in certain periods. CD, INT, and CF are shaded as blue, purple, and gray, respectively. Blank gaps denote background which is not shown.~~

360

Notably, N-containing compounds were significant in CD, such as $C_{12}H_{23}N$ and $C_7H_{12}N_2$. $C_{12}H_{23}N$ may be a compound with a pyrrole structure. Pyrrole-derived SOA may contribute to brown carbon chromophore and influence radiative forcing (Chen et al., 2024). $C_7H_{12}N_2$ (enriched in CE2) is likely 1-butyylimidazole, a derivative of imidazole, reported in reactions of methylglyoxal and amines in cloud simulation in De Haan et al. (2011). This compound has been observed from emissions of residential cooking and agricultural residual burning (Fleming et al., 2018; Wang et al., 2017; Lin et al., 2012). Moreover, imidazole has been reported as a type of brown carbon influencing regional radiative forcing (Kim et al., 2019; Lian et al., 2020; Gan et al., 2024) and may contribute to reactive oxygenated species, potentially relating to adverse health effects (Dou et al., 2015). The enhanced concentration of N-containing compounds in cloud droplets could therefore have significant atmospheric implications and warrants further investigation.

365



370

Figure 6. Typical time series of compounds: carboxylic acid ($C_2H_2O_4$), $C_6H_{12}O_6$, N-containing substances including $C_7H_{12}N_2$ and $C_{12}H_{23}N$, in a cloud episode. CD, INT, and CF are shaded as blue, purple, and gray, respectively. Gaps in the time series represent EESI-ToF-MS background measurement periods, which are not shown.

375 3.4 Dynamic variation of OA in clouds

Relatively stable T, wind speed WS, and CO concentration in a typical 3-day cloud indicate this that the cloud was stable and sources of primary emission sources remained relatively largely constant during throughout the whole cloud episode, as. The time series of CHO, CHON, and Others are shown in Fig. 7. CHO and CHON were the major constituents for most time of the episode, whereas Others was the lowest. The O/N ratio was generally lower in CD than in INT, while the ratio of O/C and N/C varied irregularly in CD and INT. Although the time resolution of our measurement (~ 20 s) is enough to capture the evolution of a compound in clouds, either in CD or INT, there was no clear trend in the time series of the compounds, either from the fractions of OA classes or elemental ratios during the sample types of CD or INT. This phenomenon is likely due to the dynamic characteristics of clouds, in which turbulence and chemical processes continuously induced rapid changes in organic compounds, resulting in no gradual trends in their concentrations.

385

From the perspective of the molecular composition, the relative intensities of representative compounds in cloud episodes exhibited frequent and pronounced fluctuations during individual CD periods, as shown in Fig. 6. Even within a 1-h CD, the signal of compounds increased and decreased irregularly, likely due to turbulence. Consequently, it is difficult to track and capture information on the chemical transformation of OA in clouds. Most previous comparisons of the chemical composition of cloud droplets with cloud-free aerosol particles or interstitial aerosol particles are based on long sampling (hours to a day) and offline analysis (Brege et al., 2018; Sun et al., 2021; Liu et al., 2023b). Based on the findings in this study, the results obtained using methods with low time resolution may be subject to uncertainties due to the dynamic nature of clouds.

390

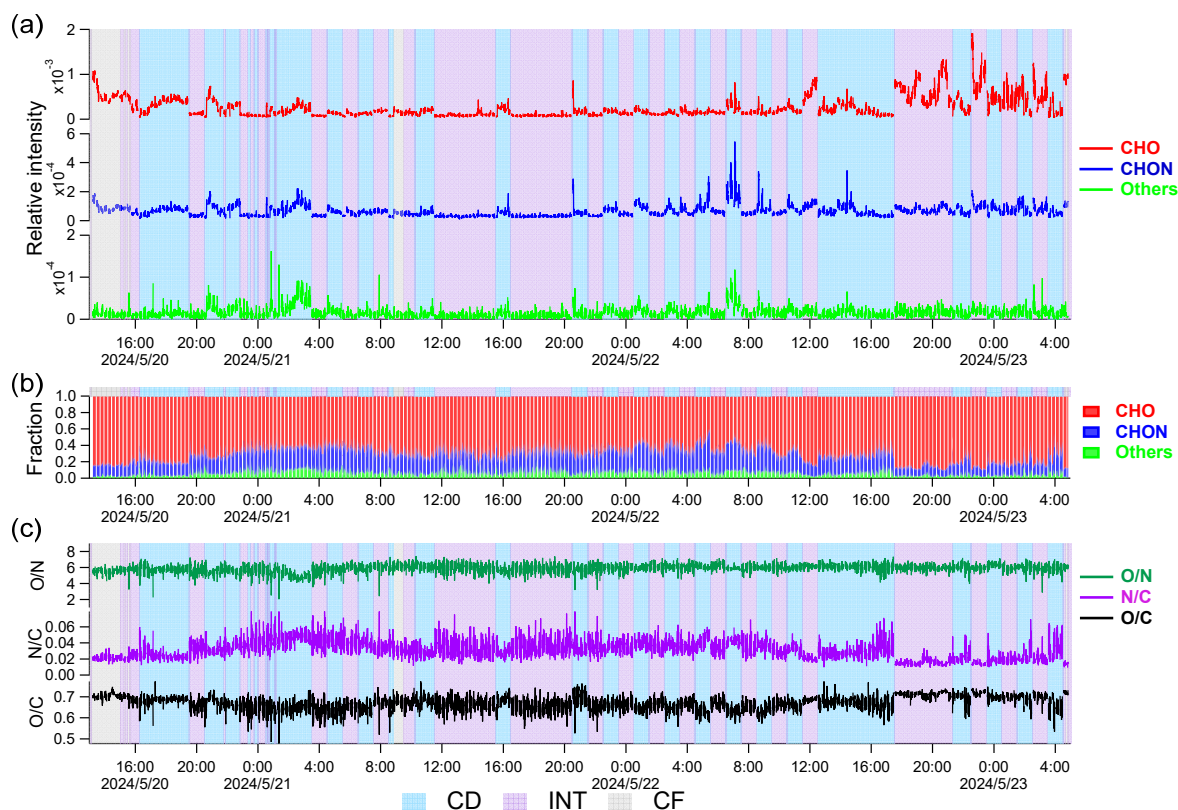


Figure 7. Time series of three classes of organic compounds (CHO, CHON₂ and Others) in a long cloud. (a) relative intensity, (b) fraction in OA, (c) O/N, N/C, and O/C ratio of OA. Blank gaps denote background data of EESI-ToF-MS, which is not shown. CD, INT, and CF are shaded in blue, purple, and gray, respectively. Gaps in the time series represent EESI-ToF-MS background measurement periods, which are not shown.

4 Conclusions and implications

In this study, we investigated aqSOA molecular composition and processing in cloud episodes we studied using online molecular information (time resolution of 20 s) obtained by EESI-ToF-MS at a high-mountain site in China. Among various classes of compounds, Cloud processing substantially influences OA composition, resulting in large differences among distinct cloud episodes. Organics in cloud droplets had an average molecular formula $C_{9.95-12.92}H_{14.53-21.78}O_{5.15-6.02}N_{0.32-0.42}S_{0.01}Si_{0-1.29}$ for the selected four cloud episodes. CHO compounds contributed predominantly to OA in cloud droplets. CHON was enhanced markedly in cloud droplets compared with cloud-free aerosol particles and interstitial aerosol particles- in most cloud episodes. The majority of CHON compounds were likely organonitrates, highlighting the enrichment of these organonitrates compounds in cloud processing. Organics OA in cloud droplets had an average molecular formula $C_{10.01-12.81}H_{14.59-20.34}O_{5.08-6.00}N_{0.34-0.43}S_{0-0.01}Si_{0-1.07}$ for the selected four cloud episodes. OA in CD had more carbon, oxygen, and nitrogen contained higher numbers of C, O, and N atoms, exhibited a CH₂-based homologous series, and showed an enrichment of higher-molecular-weight compounds compared to adjacent cloud-free aerosol particles. Organics in cloud droplets showed a homologue pattern with increasing CH₂, and larger compounds (with higher carbon number) were enriched in cloud

~~droplets compared with cloud-free aerosol particles, indicating, collectively highlighting~~ the importance of accretion reactions in cloud processing of OA.

~~at the molecular level.~~ We identified several compounds ~~that were~~ significantly enriched in cloud droplets, ~~which include some including~~ typical aqSOA tracers such as oxalic acid ~~and new compounds such as~~ $C_6H_{12}O_6$, $C_9H_{22}N_2O_4$, and $C_{12}H_{23}N$,
415 ~~etc., that can be used as aqSOA tracers. Nitrogen-containing compounds, including~~ $C_7H_{12}N_2$ and $C_{12}H_{23}N$, were observed to be enriched in cloud droplets compared with cloud-free aerosol particles. Besides, cloud processing substantially influences OA composition, resulting in large difference among distinct CEs. Based on measurement of high time resolution (~ 20 s), we find that the concentrations of individual organic compounds were highly dynamic in cloud, which is likely due to the turbulence in cloud. Such a highly dynamic nature in cloud poses difficulties in extracting the influence of chemical processes
420 ~~on individual compounds for instrumentation with low time resolution.~~ The new aqSOA tracers, such as $C_6H_{12}O_6$ and $C_9H_{22}N_2O_4$, could help future studies identify cloud processing aqSOA.

~~Our study highlights the importance of accretion reactions in cloud processing of OA. This study provides direct molecular-level evidence for the contribution of accretion reactions during cloud processing of OA. Although previous cloud observations using FT-ICR-MS reported the presence of oligomers in cloud samples, these studies could not distinguish~~
425 ~~whether such compounds originated from cloud processing or aqueous aerosols, as no concomitant aerosol samples were collected for comparison (Zhao et al., 2013; Cook et al., 2017). By directly comparing OA composition in cloud droplets with that in cloud-free aerosol particles, our results clearly demonstrate that accretion reactions occur within cloud droplets. It has been assumed that HMWC are predominantly formed in aerosol liquid water rather than cloud water, owing to the lower reaction rates of accretion reactions in the more dilute cloud-water environment (Ervens et al., 2011). In contrast, our study~~
430 ~~provides direct molecular-level evidence that such compounds can also be formed in cloud water, extending earlier observations by Cook et al. (2017). These findings highlight that accretion reactions should be considered when modeling aqSOA formation in clouds.~~

~~The HMWC formed via accretion reaction may have implications for the environment and climate.~~ Due to the increase in the ~~large-molecular-weight compounds~~ HMWC, accretion reactions likely reduce the volatility of organics and could
435 potentially enhance OA mass concentration and alter the aerosol size distribution after cloud evaporation. The formation of ~~larger compounds~~ HMWC can also modify ~~other~~ physicochemical properties, such as lifetime, oxidation state, viscosity, and hygroscopic properties, which may further influence the cloud activation of these aerosols. In addition, the formation of N-containing compounds in cloud droplets, such as organonitrates, pyrrole, and imidazole, may also affect the physicochemical properties of aqSOA, e.g., contributing to brown carbon and thus affecting regional radiative forcing.

440 ~~The new tracers of cloud processing found~~ Based on the measurement of high time resolution (~20 s), we find that the
concentrations of individual organic compounds were highly dynamic in this study, such as C₆H₁₂O₆, could help future studies
identify aqSOA processed from cloud processing. Moreover, ~~clouds~~, which is likely due to the turbulence in clouds. Such a
highly dynamic nature in clouds poses difficulties in extracting the influence of chemical processes on individual compounds
for instrumentation with low temporal resolution. Therefore, our results highlight the necessity of high time resolution
445 measurements (< 1 h), especially online ~~measurements (time)~~ systems achieving minute-level resolution of minutes) of cloud
~~droplets~~ to investigate the chemical processes in ~~cloud~~ clouds, considering dynamic variations of compounds in ~~cloud~~ clouds
due to turbulence in clouds and ~~changes~~ alterations in air masses.

It should be noted that this study provides molecular formulas only, while detailed structural information is warranted to better constrain the sources, formation mechanisms, and climate impacts of aqSOA in clouds. In addition, sources of compounds enriched in cloud droplets will be investigated in future studies.

Data availability. The data used in this study are available from the corresponding authors upon request: Defeng Zhao (dfzhao@fudan.edu.cn).

455 **Supplement.**

Author contributions. DZ conceptualized the research. YJ conducted the measurements with the aid of HL, DZ, ST, SX, and CN. XiaocP and GZ conducted GCVI measurements. XiaolP conducted the meteorological measurements. WX, YZ, YS, QC and LL provided support for sampling and operation of the Shanghuang site. YJ processed data and wrote the manuscript. YJ and DZ edited the manuscript with the inputs of all authors.

460 **Competing interests.** ~~The contact author has declared that none of the authors has any competing interests.~~ [Qi Chen is a member of the editorial board of ACP.](#)

Financial support. This work is supported by the National Natural Science Foundation of China (No. 42575109), Shanghai Pilot Program for Basic Research-Fudan University (No. 21TQ1400100 (22TQ010)), ~~and~~ the National Natural Science Foundation of China (No. 42330605), [and “Island Atmosphere and Ecology” Category IV Peak Discipline.](#)

465 **Acknowledgement.** The authors gratefully acknowledge the NOAA Air Resources Laboratory (ARL) for the provision of the HYSPLIT transport and dispersion model and/or READY website (<https://www.ready.noaa.gov>) used in this publication.

References

- Altieri, K. E., Seitzinger, S. P., Carlton, A. G., Turpin, B. J., Klein, G. C., and Marshall, A. G.: Oligomers formed through in-
cloud methylglyoxal reactions: Chemical composition, properties, and mechanisms investigated by ultra-high resolution
470 FT-ICR mass spectrometry, *Atmos. Environ.*, 42, 1476-1490, <https://doi.org/10.1016/j.atmosenv.2007.11.015>, 2008.
- Barber, V. P., LeMar, L. N., Li, Y., Zheng, J. W., Keutsch, F. N., and Kroll, J. H.: Enhanced Organic Nitrate Formation from Peroxy Radicals in the Condensed Phase, *Environ. Sci. Technol. Lett.*, 11, 975-980, <https://doi.org/10.1021/acs.estlett.4c00473>, 2024.
- 475 Bianco, A., Riva, M., Baray, J. L., Ribeiro, M., Chaumerliac, N., George, C., Bridoux, M., and Deguillaume, L.: Chemical Characterization of Cloudwater Collected at Puy de Dome by FT-ICR MS Reveals the Presence of SOA Components, *ACS Earth Space Chem.*, 3, 2076-2087, <https://doi.org/10.1021/acsearthspacechem.9b00153>, 2019.
- Boone, E. J., Laskin, A., Laskin, J., Wirth, C., Shepson, P. B., Stirm, B. H., and Pratt, K. A.: Aqueous Processing of Atmospheric Organic Particles in Cloud Water Collected via Aircraft Sampling, *Environ. Sci. Technol.*, 49, 8523-8530, <https://doi.org/10.1021/acs.est.5b01639>, 2015.
- 480 Brege, M., Paglione, M., Gilardoni, S., Decesari, S., Facchini, M. C., and Mazzoleni, L. R.: Molecular insights on aging and aqueous-phase processing from ambient biomass burning emissions-influenced Po Valley fog and aerosol, *Atmos. Chem. Phys.*, 18, 13197-13214, <https://doi.org/10.5194/acp-18-13197-2018>, 2018.
- [Brown, W. L., Day, D. A., Stark, H., Pagonis, D., Krechmer, J. E., Liu, X., Price, D. J., Katz, E. F., DeCarlo, P. F., Masoud, C. G., Wang, D. S., Hildebrandt Ruiz, L., Arata, C., Lunderberg, D. M., Goldstein, A. H., Farmer, D. K., Vance, M. E., and Jimenez, J. L.: Real-time organic aerosol chemical speciation in the indoor environment using extractive electrospray ionization mass spectrometry, *Indoor Air*, 31, 141-155, <https://doi.org/10.1111/ina.12721>, 2021.](#)
- Chen, K., Hamilton, C., Ries, B., Lum, M., Mayorga, R., Tian, L., Bahreini, R., Zhang, H., and Lin, Y. H.: Relative Humidity

- y Modulates the Physicochemical Processing of Secondary Brown Carbon Formation from Nighttime Oxidation of Furan and Pyrrole, ACS EST Air, 1, 426-437, <https://doi.org/10.1021/acsestair.4c00025>, 2024.
- Collett, J. L., Herekes, P., Youngster, S., and Lee, T.: Processing of atmospheric organic matter by California radiation fogs, Atmos. Res., 87, 232-241, <https://doi.org/10.1016/j.atmosres.2007.11.005>, 2008.
- Cook, R. D., Lin, Y. H., Peng, Z., Boone, E., Chu, R. K., Dukett, J. E., Gunsch, M. J., Zhang, W., Tolic, N., Laskin, A., and Pratt, K. A.: Biogenic, urban, and wildfire influences on the molecular composition of dissolved organic compounds in cloud water, Atmos. Chem. Phys., 17, 15167-15180, <https://doi.org/10.5194/acp-17-15167-2017>, 2017.
- Dadashazar, H., Corral, A. F., Crosbie, E., Dmitrovic, S., Kirschler, S., McCauley, K., Moore, R., Robinson, C., Schlosser, J. S., Shook, M., Thornhill, K. L., Voigt, C., Winstead, E., Ziemba, L., and Sorooshian, A.: Organic enrichment in droplet residual particles relative to out of cloud over the northwestern Atlantic: analysis of airborne ACTIVATE data, Atmos. Chem. Phys., 22, 13897-13913, <https://doi.org/10.5194/acp-22-13897-2022>, 2022.
- de Gouw, J. A., Middlebrook, A. M., Warneke, C., Goldan, P. D., Kuster, W. C., Roberts, J. M., Fehsenfeld, F. C., Worsnop, D. R., Canagaratna, M. R., Pszenny, A. A. P., Keene, W. C., Marchewka, M., Bertman, S. B., and Bates, T. S.: Budget of organic carbon in a polluted atmosphere: Results from the New England Air Quality Study in 2002, J. Geophys. Res.-Atmos., 110, <https://doi.org/10.1029/2004jd005623>, 2005.
- De Haan, D. O., Hawkins, L. N., Kononenko, J. A., Turley, J. J., Corrigan, A. L., Tolbert, M. A., and Jimenez, J. L.: Formation of Nitrogen-Containing Oligomers by Methylglyoxal and Amines in Simulated Evaporating Cloud Droplets, Environ. Sci. Technol., 45, 984-991, <https://doi.org/10.1021/es102933x>, 2011.
- Dou, J., Lin, P., Kuang, B.-Y., and Yu, J. Z.: Reactive Oxygen Species Production Mediated by Humic-like Substances in Atmospheric Aerosols: Enhancement Effects by Pyridine, Imidazole, and Their Derivatives, Environ. Sci. Technol., 49, 6457-6465, <https://doi.org/10.1021/es5059378>, 2015.
- Duan, J., Huang, R.-J., Gu, Y., Lin, C., Zhong, H., Wang, Y., Yuan, W., Ni, H., Yang, L., Chen, Y., Worsnop, D. R., and O'Dowd, C.: The formation and evolution of secondary organic aerosol during summer in Xi'an: Aqueous phase processing in fog-rain days, Sci. Total Environ., 756, <https://doi.org/10.1016/j.scitotenv.2020.144077>, 2021.
- Duan, J., Huang, R.-J., Gu, Y., Lin, C., Zhong, H., Xu, W., Liu, Q., You, Y., Ovadnevaite, J., Ceburnis, D., Hoffmann, T., and O'Dowd, C.: Measurement report: Large contribution of biomass burning and aqueous-phase processes to the wintertime secondary organic aerosol formation in Xi'an, Northwest China, Atmos. Chem. Phys., 22, 10139-10153, <https://doi.org/10.5194/acp-22-10139-2022>, 2022.
- Ervens, B., Turpin, B. J., and Weber, R. J.: Secondary organic aerosol formation in cloud droplets and aqueous particles (aqSOA): a review of laboratory, field and model studies, Atmos. Chem. Phys., 11, 11069-11102, <https://doi.org/10.5194/acp-11-11069-2011>, 2011.
- Fenselau, R. Z., Alotbi, A. R., Lee, C. B., Cronin, J. S., Hill, D. R., Belitsky, J. M., and Elrod, M. J.: A New Potential Atmospheric Accretion Mechanism: Acid-Catalyzed Hetero-Michael Addition Reactions, ACS Earth Space Chem., 9, 191-200, <https://doi.org/10.1021/acsearthspacechem.4c00342>, 2025.
- Fleming, L. T., Lin, P., Laskin, A., Laskin, J., Weltman, R., Edwards, R. D., Arora, N. K., Yadav, A., Meinardi, S., Blake, D. R., Pillarisetti, A., Smith, K. R., and Nizkorodov, S. A.: Molecular composition of particulate matter emissions from dung and brushwood burning household cookstoves in Haryana, India, Atmos. Chem. Phys., 18, 2461-2480, <https://doi.org/10.5194/acp-18-2461-2018>, 2018.
- Fu, T.-M., Jacob, D. J., Wittrock, F., Burrows, J. P., Vrekoussis, M., and Henze, D. K.: Global budgets of atmospheric glyoxal and methylglyoxal, and implications for formation of secondary organic aerosols, J. Geophys. Res., 113, D15303, <https://doi.org/10.1029/2007jd009505>, 2008.
- Galloway, J. N., Likens, G. E., and Edgerton, E. S.: Acid Precipitation In the Northeastern United States: pH and Acidity, Science, 194, 722-724, <https://doi.org/10.1126/science.194.4266.722>, 1976.
- Gan, Y., Lu, X., Chen, S., Jiang, X., Yang, S., Ma, X., Li, M., Yang, F., Shi, Y., and Wang, X.: Aqueous-phase formation of N-containing secondary organic compounds affected by the ionic strength, J Environ Sci (China), 138, 88-101, <https://doi.org/10.1016/j.jes.2020.08.011>, 2020.

[oi.org/10.1016/j.jes.2023.03.003](https://doi.org/10.1016/j.jes.2023.03.003), 2024.

- 535 Gao, M., Zhou, S., He, Y., Zhang, G., Ma, N., Li, Y., Li, F., Yang, Y., Peng, L., Zhao, J., Bi, X., Hu, W., Sun, Y., Wang, B.,
and Wang, X.: In Situ Observation of Multiphase Oxidation-Driven Secondary Organic Aerosol Formation during Clou
d Processing at a Mountain Site in Southern China, *Environ. Sci. Technol. Lett.*, 10, 573–581, [https://doi.org/10.1021/ac
s.estlett.3c00331](https://doi.org/10.1021/ac
s.estlett.3c00331), 2023.
- 540 Gilardoni, S., Massoli, P., Paglione, M., Giulianelli, L., Carbone, C., Rinaldi, M., Decesari, S., Sandrini, S., Costabile, F., Go
bbi, G. P., Pietrogrande, M. C., Visentin, M., Scotto, F., Fuzzi, S., and Facchini, M. C.: Direct observation of aqueous se
condary organic aerosol from biomass-burning emissions, *Proc. Natl. Acad. Sci. U. S. A.*, 113, 10013-10018, [https://doi
.org/10.1073/pnas.1602212113](https://doi
.org/10.1073/pnas.1602212113), 2016.
- 545 [Gkatzelis, G. I., Coggon, M. M., McDonald, B. C., Peischl, J., Gilman, J. B., Aikin, K. C., Robinson, M. A., Canonaco, F., P
revot, A. S. H., Trainer, M., and Warneke, C.: Observations Confirm that Volatile Chemical Products Are a Major Sour
ce of Petrochemical Emissions in U.S. Cities, *Environ. Sci. Technol.*, 55, 4332–4343, \[https://doi.org/10.1021/acs.est.0c0
5471\]\(https://doi.org/10.1021/acs.est.0c0
5471\), 2021.](https://doi.org/10.1021/acs.est.0c05471)
- [Graedel, T. E. and Weschler, C. J.: Chemistry Within Aqueous Atmospheric Aerosols And Raindrops, *Reviews of Geophysi
cs*, 19, 505-539, <https://doi.org/10.1029/RG019i004p00505>, 1981.](https://doi.org/10.1029/RG019i004p00505)
- 550 Gramlich, Y., Siegel, K., Haslett, S. L., Freitas, G., Krejci, R., Zieger, P., and Mohr, C.: Revealing the chemical characteristi
cs of Arctic low-level cloud residuals – in situ observations from a mountain site, *Atmos. Chem. Phys.*, 23, 6813-6834,
<https://doi.org/10.5194/acp-23-6813-2023>, 2023.
- Guo, Y., Shen, H., Pullinen, I., Luo, H., Kang, S., Vereecken, L., Fuchs, H., Hallquist, M., Acir, I.-H., Tillmann, R., Rohrer,
F., Wildt, J., Kiendler-Scharr, A., Wahner, A., Zhao, D., and Mentel, T. F.: Identification of highly oxygenated organic
molecules and their role in aerosol formation in the reaction of limonene with nitrate radical, *Atmos. Chem. Phys.*, 22, 1
1323-11346, <https://doi.org/10.5194/acp-22-11323-2022>, 2022.
- 555 [Hao, Y., Strahl, J., Khare, P., Cui, T., Schneider-Beltran, K., Qi, L., Wang, D., Top, J., Surdu, M., Bhattu, D., Bhowmik, H.
S., Vats, P., Rai, P., Kumar, V., Ganguly, D., Szidat, S., Uzu, G., Jaffrezou, J. L., Elazzouzi, R., Rastogi, N., Slowik, J., H
addad, I. E., Tripathi, S. N., Prevot, A. S. H., and Daellenbach, K. R.: Transported smoke from crop residue burning as t
he major source of organic aerosol and health risks in northern Indian cities during post-monsoon, *Environ Int*, 202, 109
583, <https://doi.org/10.1016/j.envint.2025.109583>, 2025.](https://doi.org/10.1016/j.envint.2025.109583)
- 560 [Herckes, P., Valsaraj, K. T., and Collett, J. L., Jr.: A review of observations of organic matter in fogs and clouds: Origin, pro
cessing and fate, *Atmos. Res.*, 132, 434-449, <https://doi.org/10.1016/j.atmosres.2013.06.005>, 2013.](https://doi.org/10.1016/j.atmosres.2013.06.005)
- Huang, W., Huang, R. J., Duan, J., Lin, C., Zhong, H., Xu, W., Gu, Y., Ni, H., Chang, Y., and Wang, X.: Size-Dependent Ni
ghttime Formation of Particulate Secondary Organic Nitrates in Urban Air, *J. Geophys. Res.-Atmos.*, 128, [https://doi.or
g/10.1029/2022jd038189](https://doi.or
g/10.1029/2022jd038189), 2023.
- 565 Jimenez, J. L., Canagaratna, M. R., Donahue, N. M., Prevot, A. S. H., Zhang, Q., Kroll, J. H., DeCarlo, P. F., Allan, J. D., Co
e, H., Ng, N. L., Aiken, A. C., Docherty, K. S., Ulbrich, I. M., Grieshop, A. P., Robinson, A. L., Duplissy, J., Smith, J.
D., Wilson, K. R., Lanz, V. A., Hueglin, C., Sun, Y. L., Tian, J., Laaksonen, A., Raatikainen, T., Rautiainen, J., Vaattov
aara, P., Ehn, M., Kulmala, M., Tomlinson, J. M., Collins, D. R., Cubison, M. J., Dunlea, E. J., Huffman, J. A., Onasch,
570 T. B., Alfarra, M. R., Williams, P. I., Bower, K., Kondo, Y., Schneider, J., Drewnick, F., Borrmann, S., Weimer, S., De
merjian, K., Salcedo, D., Cottrell, L., Griffin, R., Takami, A., Miyoshi, T., Hatakeyama, S., Shimono, A., Sun, J. Y., Zh
ang, Y. M., Dzepina, K., Kimmel, J. R., Sueper, D., Jayne, J. T., Herndon, S. C., Trimborn, A. M., Williams, L. R., Woo
d, E. C., Middlebrook, A. M., Kolb, C. E., Baltensperger, U., and Worsnop, D. R.: Evolution of Organic Aerosols in the
Atmosphere, *Science*, 326, 1525-1529, <https://doi.org/10.1126/science.1180353>, 2009.
- 575 [Karlsson, L., Baccharini, A., Duplessis, P., Baumgardner, D., Brooks, I. M., Chang, R. Y. W., Dada, L., Dällenbach, K. R., He
ikkinen, L., Krejci, R., Leaitch, W. R., Leck, C., Partridge, D. G., Salter, M. E., Wernli, H., Wheeler, M. J., Schmale, J.,
and Zieger, P.: Physical and Chemical Properties of Cloud Droplet Residuals and Aerosol Particles During the Arctic O
cean 2018 Expedition, *J. Geophys. Res. Atmos.*, 127, <https://doi.org/10.1029/2021jd036383>, 2022.](https://doi.org/10.1029/2021jd036383)

- Kim, H., Collier, S., Ge, X., Xu, J., Sun, Y., Jiang, W., Wang, Y., Herckes, P., and Zhang, Q.: Chemical processing of water-soluble species and formation of secondary organic aerosol in fogs, *Atmos. Environ.*, 200, 158-166, <https://doi.org/10.1016/j.atmosenv.2018.11.062>, 2019.
- Kumar, V., Giannoukos, S., Haslett, S. L., Tong, Y., Singh, A., Bertrand, A., Lee, C. P., Wang, D. S., Bhattu, D., Stefenelli, G., Dave, J. S., Puthussery, J. V., Qi, L., Vats, P., Rai, P., Casotto, R., Satish, R., Mishra, S., Pospisilova, V., Mohr, C., Bell, D. M., Ganguly, D., Verma, V., Rastogi, N., Baltensperger, U., Tripathi, S. N., Prévôt, A. S. H., and Slowik, J. G.: Highly time-resolved chemical speciation and source apportionment of organic aerosol components in Delhi, India, using extractive electrospray ionization mass spectrometry, *Atmos. Chem. Phys.*, 22, 7739-7761, <https://doi.org/10.5194/acp-22-7739-2022>, 2022.
- Lamkaddam, H., Dommen, J., Ranjithkumar, A., Gordon, H., Wehrle, G., Krechmer, J., Majluf, F., Salionov, D., Schmale, J., Bjelic, S., Carslaw, K. S., El Haddad, I., and Baltensperger, U.: Large contribution to secondary organic aerosol from isoprene cloud chemistry, *Sci. Adv.*, 7, eabe2952, <https://doi.org/10.1126/sciadv.abe2952>, 2021.
- Lance, S., Zhang, J., Schwab, J. J., Casson, P., Brandt, R. E., Fitzjarrald, D. R., Schwab, M. J., Sicker, J., Lu, C. H., Chen, S. P., Yun, J., Freedman, J. M., Shrestha, B., Min, Q. L., Beauharnois, M., Crandall, B., Joseph, E., Brewer, M. J., Minder, J. R., Orłowski, D., Christiansen, A., Carlton, A. G., and Barth, M. C.: Overview of the CPOC Pilot Study at Whiteface Mountain, NY Cloud Processing of Organics within Clouds (CPOC), *Bull. Amer. Meteorol. Soc.*, 101, E1820-E1841, <https://doi.org/10.1175/bams-d-19-0022.1>, 2020.
- LeClair, J. P., Collett, J. L., and Mazzoleni, L. R.: Fragmentation Analysis of Water-Soluble Atmospheric Organic Matter Using Ultrahigh-Resolution FT-ICR Mass Spectrometry, *Environ. Sci. Technol.*, 46, 4312-4322, <https://doi.org/10.1021/es203509b>, 2012.
- Li, Y., Fu, T. M., Yu, J. Z., Yu, X., Chen, Q., Miao, R., Zhou, Y., Zhang, A., Ye, J., Yang, X., Tao, S., Liu, H., and Yao, W.: Dissecting the contributions of organic nitrogen aerosols to global atmospheric nitrogen deposition and implications for ecosystems, *Natl Sci Rev.*, 10, nwad244, <https://doi.org/10.1093/nsr/nwad244>, 2023.
- Li, Z., Schwier, A. N., Sareen, N., and McNeill, V. F.: Reactive processing of formaldehyde and acetaldehyde in aqueous aerosol mimics: surface tension depression and secondary organic products, *Atmos. Chem. Phys.*, 11, 11617-11629, <https://doi.org/10.5194/acp-11-11617-2011>, 2011.
- Lian, X., Zhang, G., Yang, Y., Lin, Q., Fu, Y., Jiang, F., Peng, L., Hu, X., Chen, D., Wang, X., Peng, P. a., Sheng, G., and Bi, X.: Evidence for the Formation of Imidazole from Carbonyls and Reduced Nitrogen Species at the Individual Particle Level in the Ambient Atmosphere, *Environ. Sci. Technol. Lett.*, 8, 9-15, <https://doi.org/10.1021/acs.estlett.0c00722>, 2020.
- Lim, Y. B., Tan, Y., Perri, M. J., Seitzinger, S. P., and Turpin, B. J.: Aqueous chemistry and its role in secondary organic aerosol (SOA) formation, *Atmos. Chem. Phys.*, 10, 10521-10539, <https://doi.org/10.5194/acp-10-10521-2010>, 2010.
- Lin, P., Rincon, A. G., Kalberer, M., and Yu, J. Z.: Elemental Composition of HULIS in the Pearl River Delta Region, China: Results Inferred from Positive and Negative Electrospray High Resolution Mass Spectrometric Data, *Environ. Sci. Technol.*, 46, 7454-7462, <https://doi.org/10.1021/es300285d>, 2012.
- Lin, Q., Zhang, G., Peng, L., Bi, X., Wang, X., Brechtel, F. J., Li, M., Chen, D., Peng, P. a., Sheng, G., and Zhou, Z.: In situ chemical composition measurement of individual cloud residue particles at a mountain site, southern China, *Atmos. Chem. Phys.*, 17, 8473-8488, <https://doi.org/10.5194/acp-17-8473-2017>, 2017.
- Liu, B., Li, Q., Sun, R., Dong, R., Wang, S., and Hao, J.: Pollution Characteristics and Factors Influencing the Reduction of Ambient PM_{2.5} in Beijing from 2018 to 2020, *Huanjing Kexue*, 44, 2409-2420, <https://doi.org/10.13227/j.hjcx.202205244>, 2023a.
- Liu, Z., Zhu, B., Zhu, C., Ruan, T., Li, J., Chen, H., Li, Q., Wang, X., Wang, L., Mu, Y., Collett, J., George, C., Wang, Y., Wang, X., Su, J., Yu, S., Mellouki, A., Chen, J., and Jiang, G.: Abundant nitrogenous secondary organic aerosol formation accelerated by cloud processing, *iScience*, 26, 108317, <https://doi.org/10.1016/j.isci.2023.108317>, 2023b.
- Lopez-Hilfiker, F. D., Pospisilova, V., Huang, W., Kalberer, M., Mohr, C., Stefenelli, G., Thornton, J. A., Baltensperger, U.,

- 625 Prevo, A. S. H., and Slowik, J. G.: An extractive electrospray ionization time-of-flight mass spectrometer (EESI-TOF) for online measurement of atmospheric aerosol particles, *Atmos. Meas. Tech.*, 12, 4867-4886, <https://doi.org/10.5194/amt-12-4867-2019>, 2019.
- Luo, H., Guo, Y., Shen, H., Huang, D. D., Zhang, Y., and Zhao, D.: Effect of relative humidity on the molecular composition of secondary organic aerosols from α -pinene ozonolysis, *Environ. Sci. - Atmospheres*, 4, 519-530, <https://doi.org/10.1039/d3ea00149k>, 2024.
- 630 ~~McDonald, B. C., de Gouw, J. A., Gilman, J. B., Jathar, S. H., Akherati, A., Cappa, C. D., Jimenez, J. L., Lee Taylor, J., Hayes, P. L., McKeen, S. A., Cui, Y. Y., Kim, S. W., Gentner, D. R., Isaacman VanWertz, G., Goldstein, A. H., Harley, R. A., Frost, G. J., Roberts, J. M., Ryerson, T. B., and Trainer, M.: Volatile chemical products emerging as largest petrochemical source of urban organic emissions, *Science*, 359, 760-764, <https://doi.org/10.1126/science.aag0524>, 2018.~~
- 635 ~~Mandariya, A. K., Gupta, T., and Tripathi, S. N.: Effect of aqueous-phase processing on the formation and evolution of organic aerosol (OA) under different stages of fog life cycles, *Atmos. Environ.*, 206, 60-71, <https://doi.org/10.1016/j.atmosenv.2019.02.047>, 2019.~~
- ~~Mattsson, F., Neuberger, A., Heikkinen, L., Gramlich, Y., Paglione, M., Rinaldi, M., Decesari, S., Zieger, P., Riipinen, I., and Mohr, C.: Enrichment of organic nitrogen in fog residuals observed in the Italian Po Valley, *Atmos. Chem. Phys.*, 25, 7973-7989, <https://doi.org/10.5194/acp-25-7973-2025>, 2025.~~
- 640 ~~Mayhew, A. W., Franzon, L., Bates, K. H., Kurtén, T., Lopez-Hilfiker, F. D., Mohr, C., Rickard, A. R., Thornton, J. A., and Haskins, J. D.: The global importance of gas-phase peroxy radical accretion reactions for secondary organic aerosol loading, *Atmos. Chem. Phys.*, 25, 17027-17046, <https://doi.org/10.5194/acp-25-17027-2025>, 2025.~~
- McNeill, V. F.: Aqueous organic chemistry in the atmosphere: sources and chemical processing of organic aerosols, *Environ. Sci. Technol.*, 49, 1237-1244, <https://doi.org/10.1021/es5043707>, 2015.
- 645 McNeill, V. F., Woo, J. L., Kim, D. D., Schwier, A. N., Wannell, N. J., Sumner, A. J., and Barakat, J. M.: Aqueous-Phase Secondary Organic Aerosol and Organosulfate Formation in Atmospheric Aerosols: A Modeling Study, *Environ. Sci. Technol.*, 46, 8075-8081, <https://doi.org/10.1021/es3002986>, 2012.
- ~~Motos, G., Schmale, J., Corbin, J. C., Modini, R. L., Karlen, N., Bertò, M., Baltensperger, U., and Gysel Beer, M.: Cloud droplet activation properties and scavenged fraction of black carbon in liquid phase clouds at the high alpine research station Jungfraujoch (3580 m a.s.l.), *Atmos. Chem. Phys.*, 19, 3833-3855, <https://doi.org/10.5194/acp-19-3833-2019>, 2019.~~
- 650 Nault, B. A., Jo, D. S., McDonald, B. C., Campuzano-Jost, P., Day, D. A., Hu, W., Schroder, J. C., Allan, J., Blake, D. R., Canagaratna, M. R., Coe, H., Coggon, M. M., DeCarlo, P. F., Diskin, G. S., Dunmore, R., Flocke, F., Fried, A., Gilman, J. B., Gkatzelis, G., Hamilton, J. F., Hanisco, T. F., Hayes, P. L., Henze, D. K., Hodzic, A., Hopkins, J., Hu, M., Huey, L. G., Jobson, B. T., Kuster, W. C., Lewis, A., Li, M., Liao, J., Nawaz, M. O., Pollack, I. B., Peischl, J., Rappenglück, B., Reeves, C. E., Richter, D., Roberts, J. M., Ryerson, T. B., Shao, M., Sommers, J. M., Walega, J., Warneke, C., Weibring, P., Wolfe, G. M., Young, D. E., Yuan, B., Zhang, Q., de Gouw, J. A., and Jimenez, J. L.: Secondary organic aerosols from anthropogenic volatile organic compounds contribute substantially to air pollution mortality, *Atmos. Chem. Phys.*, 21, 11201-11224, <https://doi.org/10.5194/acp-21-11201-2021>, 2021.
- 655 Ng, N. L., Brown, S. S., Archibald, A. T., Atlas, E., Cohen, R. C., Crowley, J. N., Day, D. A., Donahue, N. M., Fry, J. L., Fuhs, H., Griffin, R. J., Guzman, M. I., Herrmann, H., Hodzic, A., Iinuma, Y., Jimenez, J. L., Kiendler-Scharr, A., Lee, B. H., Luecken, D. J., Mao, J., McLaren, R., Mutzel, A., Osthoff, H. D., Ouyang, B., Picquet-Varrault, B., Platt, U., Pye, H. O. T., Rudich, Y., Schwantes, R. H., Shiraiwa, M., Stutz, J., Thornton, J. A., Tilgner, A., Williams, B. J., and Zaveri, R. A.: Nitrate radicals and biogenic volatile organic compounds: oxidation, mechanisms, and organic aerosol, *Atmos. Chem. Phys.*, 17, 2103-2162, <https://doi.org/10.5194/acp-17-2103-2017>, 2017.
- 660 Odum, J. R., Hoffmann, T., Bowman, F., Collins, D., Flagan, R. C., and Seinfeld, J. H.: Gas/particle partitioning and secondary organic aerosol yields, *Environ. Sci. Technol.*, 30, 2580-2585, <https://doi.org/10.1021/es950943>, 1996.
- Pailler, L., Deguillaume, L., Lavanant, H., Schmitz, I., Hubert, M., Nicol, E., Ribeiro, M., Pichon, J. M., Vařtilingom, M., Dominutti, P., Burnet, F., Tulet, P., Leriche, M., and Bianco, A.: Molecular composition of clouds: a comparison between s

amples collected at tropical (Réunion Island, France) and mid-north (Puy de Dôme, France) latitudes, *Atmos. Chem. Phys.*, 24, 5567-5584, <https://doi.org/10.5194/acp-24-5567-2024>, 2024.

Pasquier, J. T., David, R. O., Freitas, G., Gierens, R., Gramlich, Y., Haslett, S., Li, G., Schäfer, B., Siegel, K., Wieder, J., Adachi, K., Belosi, F., Carlsen, T., Decesari, S., Ebell, K., Gilardoni, S., Gysel-Ber, M., Henneberger, J., Inoue, J., Kanji, Z. A., Koike, M., Kondo, Y., Krejci, R., Lohmann, U., Maturilli, M., Mazzolla, M., Modini, R., Mohr, C., Motos, G., Nenes, A., Nicosia, A., Ohata, S., Paglione, M., Park, S., Pileci, R. E., Ramelli, F., Rinaldi, M., Ritter, C., Sato, K., Storelvmo, T., Tobo, Y., Traversi, R., Viola, A., and Zieger, P.: The Ny-Ålesund Aerosol Cloud Experiment (NASCENT): Overview and First Results, *Bull. Amer. Meteorol. Soc.*, 103, E2533-E2558, <https://doi.org/10.1175/bams-d-21-0034.1.2022>.

Qi, L., Chen, M., Stefenelli, G., Pospisilova, V., Tong, Y., Bertrand, A., Hueglin, C., Ge, X., Baltensperger, U., Prévôt, A. S. H., and Slowik, J. G.: Organic aerosol source apportionment in Zurich using an extractive electrospray ionization time-of-flight mass spectrometer (EESI-TOF-MS) – Part 2: Biomass burning influences in winter, *Atmos. Chem. Phys.*, 19, 8037-8062, <https://doi.org/10.5194/acp-19-8037-2019>, 2019.

Rogers, M. J., Joo, T., Hass-Mitchell, T., Canagaratna, M. R., Campuzano-Jost, P., Sueper, D., Tran, M. N., Machesky, J. E., Roscioli, J. R., Jimenez, J. L., Krechmer, J. E., Lambe, A. T., Nault, B. A., and Gentner, D. R.: Humid Summers Promote Urban Aqueous-Phase Production of Oxygenated Organic Aerosol in the Northeastern United States, *Geophys. Res. Lett.*, 52, <https://doi.org/10.1029/2024gl12005>, 2025.

Roland, D., Barbara, S., Glenn, R., Ariel, S., Albion, T., Sonny, Z., Chris, L., and Alice, C.: HYSPLIT USER'S GUIDE, 2025

Rolph, G., Stein, A., and Stunder, B.: Real-time Environmental Applications and Display sYstem: READY, *Environ. Modell. Softw.*, 95, 210-228, <https://doi.org/10.1016/j.envsoft.2017.06.025>, 2017.

Sehested, K., Christensen, H. C., Hart, E. J., and Corfitzen, H.: Rates Of Reaction Of O[•], OH, And H With Methylated Benzenes In Aqueous Solution. Optical Spectra Of Radicals, *J. Phys. Chem.*, 79, 310-315, <https://doi.org/10.1021/j100571a005>, 1975.

Shen, H., Zhao, D., Pullinen, I., Kang, S., Vereecken, L., Fuchs, H., Acir, I. H., Tillmann, R., Rohrer, F., Wildt, J., Kiendler-Scharr, A., Wahner, A., and Mentel, T. F.: Highly Oxygenated Organic Nitrates Formed from NO₃ Radical-Initiated Oxidation of β-Pinene, *Environ. Sci. Technol.*, 55, 15658-15671, <https://doi.org/10.1021/acs.est.1c03978>, 2021.

Shen, H. R., Vereecken, L., Kang, S. A., Pullinen, I., Fuchs, H., Zhao, D. F., and Mentel, T. F.: Unexpected significance of a minor reaction pathway in daytime formation of biogenic highly oxygenated organic compounds, *Sci. Adv.*, 8, eabp8702, <https://doi.org/10.1126/sciadv.abp8702>, 2022.

Shingler, T., Dey, S., Sorooshian, A., Brechtel, F. J., Wang, Z., Metcalf, A., Coggon, M., Mülmenstädt, J., Russell, L. M., Jonsson, H. H., and Seinfeld, J. H.: Characterisation and airborne deployment of a new counterflow virtual impactor inlet, *Atmos. Meas. Tech.*, 5, 1259-1269, <https://doi.org/10.5194/amt-5-1259-2012>, 2012.

Song, Z., Gao, W., Shen, H., Jin, Y., Zhang, C., Luo, H., Pan, L., Yao, B., Zhang, Y., Huo, J., Sun, Y., Yu, D., Chen, H., Chen, J., Duan, Y., Zhao, D., and Xu, J.: Roles of Regional Transport and Vertical Mixing in Aerosol Pollution in Shanghai Over the COVID-19 Lockdown Period Observed Above Urban Canopy, *J. Geophys. Res.-Atmos.*, 128, <https://doi.org/10.1029/2023jd038540>, 2023.

Stefenelli, G., Pospisilova, V., Lopez-Hilfiker, F. D., Daellenbach, K. R., Hüglin, C., Tong, Y., Baltensperger, U., Prévôt, A. S. H., and Slowik, J. G.: Organic aerosol source apportionment in Zurich using an extractive electrospray ionization time-of-flight mass spectrometer (EESI-TOF-MS) – Part 1: Biogenic influences and day–night chemistry in summer, *Atmos. Chem. Phys.*, 19, 14825-14848, <https://doi.org/10.5194/acp-19-14825-2019>, 2019.

Stein, A. F., Draxler, R. R., Rolph, G. D., Stunder, B. J. B., Cohen, M. D., and Ngan, F.: NOAA's HYSPLIT atmospheric transport and dispersion modeling system, *Bull. Amer. Meteor. Soc.*, 96, 2059-2077, <https://doi.org/10.1175/BAMS-D-14-00110.1>, 2015.

Sun, W., Hu, X., Fu, Y., Zhang, G., Zhu, Y., Wang, X., Yan, C., Xue, L., Meng, H., Jiang, B., Liao, Y., Wang, X., Peng, P. a

- ., and Bi, X.: Different formation pathways of nitrogen-containing organic compounds in aerosols and fog water in northern China, *Atmos. Chem. Phys.*, 24, 6987-6999, <https://doi.org/10.5194/acp-24-6987-2024>, 2024a.
- 715 Sun, W., Fu, Y., Zhang, G., Yang, Y., Jiang, F., Lian, X., Jiang, B., Liao, Y., Bi, X., Chen, D., Chen, J., Wang, X., Ou, J., Peng, P. a., and Sheng, G.: Measurement report: Molecular characteristics of cloud water in southern China and insights into aqueous-phase processes from Fourier transform ion cyclotron resonance mass spectrometry, *Atmos. Chem. Phys.*, 21, 16631-16644, <https://doi.org/10.5194/acp-21-16631-2021>, 2021.
- 720 Sun, W., Zhang, G., Guo, Z., Fu, Y., Peng, X., Yang, Y., Hu, X., Lin, J., Jiang, F., Jiang, B., Liao, Y., Chen, D., Chen, J., Ou, J., Wang, X., Peng, P. a., and Bi, X.: Formation of In-Cloud Aqueous-Phase Secondary Organic Matter and Related Characteristic Molecules, *J. Geophys. Res.-Atmos.*, 129, <https://doi.org/10.1029/2023jd040355>, 2024b.
- Sun, Y., [Luo, H., Li, Y., Zhou, W., Xu, W., Fu, P., and Zhao, D.: Atmospheric organic aerosols: online molecular characterization and environmental impacts, *npj Clim. Atmos. Sci.*, 8, <https://doi.org/10.1038/s41612-025-01199-2>, 2025.](https://doi.org/10.1038/s41612-025-01199-2)
- 725 [Sun, Y., Du, W., Fu, P., Wang, Q., Li, J., Ge, X., Zhang, Q., Zhu, C., Ren, L., Xu, W., Zhao, J., Han, T., Worsnop, D. R., and Wang, Z.: Primary and secondary aerosols in Beijing in winter: sources, variations and processes, *Atmos. Chem. Phys.*, 16, 8309-8329, <https://doi.org/10.5194/acp-16-8309-2016>, 2016.](https://doi.org/10.5194/acp-16-8309-2016)
- Surdu, M., Top, J., Yang, B., Zhang, J., Slowik, J. G., Prevot, A. S. H., Wang, D. S., El Haddad, I., and Bell, D. M.: Real-Time Identification of Aerosol-Phase Carboxylic Acid Production Using Extractive Electrospray Ionization Mass Spectrometry, *Environ. Sci. Technol.*, <https://doi.org/10.1021/acs.est.4c01605>, 2024.
- 730 Tan, Y., Perri, M. J., Seitzinger, S. P., and Turpin, B. J.: Effects of Precursor Concentration and Acidic Sulfate in Aqueous Glyoxal-OH Radical Oxidation and Implications for Secondary Organic Aerosol, *Environ. Sci. Technol.*, 43, 8105-8112, <https://doi.org/10.1021/es901742f>, 2009.
- [Thomas, A. E., Perraud, V., Lee, M., Rojas, B., Cooke, M. E., Wingen, L. M., Bauer, P. S., Dam, M., Finlayson-Pitts, B. J., and Smith, J. N.: Organic composition of ultrafine particles formed from automotive braking, *Environ Sci Process Impacts*, <https://doi.org/10.1039/d5em00654f>, 2025.](https://doi.org/10.1039/d5em00654f)
- 735 [Tilgner, A., Schaefer, T., Alexander, B., Barth, M., Collett, J. L., Jr., Fahey, K. M., Nenes, A., Pye, H. O. T., Herrmann, H., and McNeill, V. F.: Acidity and the multiphase chemistry of atmospheric aqueous particles and clouds, *Atmos. Chem. Phys.*, 21, 13483-13536, <https://doi.org/10.5194/acp-21-13483-2021>, 2021.](https://doi.org/10.5194/acp-21-13483-2021)
- 740 Tong, Y., Pospisilova, V., Qi, L., Duan, J., Gu, Y., Kumar, V., Rai, P., Stefanelli, G., Wang, L., Wang, Y., Zhong, H., Baltensperger, U., Cao, J., Huang, R.-J., Prévôt, A. S. H., and Slowik, J. G.: Quantification of solid fuel combustion and aqueous chemistry contributions to secondary organic aerosol during wintertime haze events in Beijing, *Atmos. Chem. Phys.*, 21, 9859-9886, <https://doi.org/10.5194/acp-21-9859-2021>, 2021.
- 745 Volkamer, R., Martini, F. S., Molina, L. T., Salcedo, D., Jimenez, J. L., and Molina, M. J.: A missing sink for gas-phase glyoxal in Mexico City: Formation of secondary organic aerosol, *Geophys. Res. Lett.*, 34, <https://doi.org/10.1029/2007gl030752>, 2007.
- Volkamer, R., Jimenez, J. L., San Martini, F., Dzepina, K., Zhang, Q., Salcedo, D., Molina, L. T., Worsnop, D. R., and Molina, M. J.: Secondary organic aerosol formation from anthropogenic air pollution: Rapid and higher than expected, *Geophys. Res. Lett.*, 33, L17811, <https://doi.org/10.1029/2006gl026899>, 2006.
- 750 Wang, J., Ye, J., Zhang, Q., Zhao, J., Wu, Y., Li, J., Liu, D., Li, W., Zhang, Y., Wu, C., Xie, C., Qin, Y., Lei, Y., Huang, X., Guo, J., Liu, P., Fu, P., Li, Y., Lee, H. C., Choi, H., Zhang, J., Liao, H., Chen, M., Sun, Y., Ge, X., Martin, S. T., and Jacob, D. J.: Aqueous production of secondary organic aerosol from fossil-fuel emissions in winter Beijing haze, *Proc. Natl. Acad. Sci. U. S. A.*, 118, e2022179118, <https://doi.org/10.1073/pnas.2022179118>, 2021.
- 755 Wang, [L., Slowik, J. G., Klein, F., Stefanelli, G., Pospisilova, V., Tong, Y., Baltensperger, U., and Prevot, A. S. H.: Characteristics of oxygenated volatile organic compounds in Zurich, Switzerland: Sources, composition, and implication for secondary aerosol formation, *Chemosphere*, 368, 143686, <https://doi.org/10.1016/j.chemosphere.2024.143686>, 2024a.](https://doi.org/10.1016/j.chemosphere.2024.143686)
- [Wang, T., Li, K., Bell, D. M., Zhang, J., Cui, T., Surdu, M., Baltensperger, U., Slowik, J. G., Lamkaddam, H., El Haddad, I., and Prevot, A. S. H.: Large contribution of in-cloud production of secondary organic aerosol from biomass burning emissions](https://doi.org/10.1021/es901742f)

- ssions, *npj Clim. Atmos. Sci.*, 7, <https://doi.org/10.1038/s41612-024-00682-6>, 2024a2024b.
- 760 Wang, Y., Hu, M., Lin, P., Guo, Q., Wu, Z., Li, M., Zeng, L., Song, Y., Zeng, L., Wu, Y., Guo, S., Huang, X., and He, L.: Molecular Characterization of Nitrogen-Containing Organic Compounds in Humic-like Substances Emitted from Straw Residue Burning, *Environ. Sci. Technol.*, 51, 5951-5961, <https://doi.org/10.1021/acs.est.7b00248>, 2017.
- Xu, W., Sun, Y., Wang, Q., Zhao, J., Wang, J., Ge, X., Xie, C., Zhou, W., Du, W., Li, J., Fu, P., Wang, Z., Worsnop, D. R., and Coe, H.: Changes in Aerosol Chemistry From 2014 to 2016 in Winter in Beijing: Insights From High-Resolution Aerosol Mass Spectrometry, *J. Geophys. Res.-Atmos.*, 124, 1132-1147, <https://doi.org/10.1029/2018jd029245>, 2019.
- 765 [Xue, S., Luo, H., Wang, Z., Shen, H., Zhang, Y., Nie, C., Song, Z., Wang, L., Wang, S., Chen, J., and Zhao, D.: Online molecular insights into sources and formation of organic aerosol in Shanghai, *npj Clim. Atmos. Sci.*, 8, <https://doi.org/10.1038/s41612-025-01230-6>, 2025.](https://doi.org/10.1038/s41612-025-01230-6)
- Yin, C., Xu, J., Gao, W., Pan, L., Gu, Y., Fu, Q., and Yang, F.: Characteristics of fine particle matter at the top of Shanghai Tower, *Atmos. Chem. Phys.*, 23, 1329-1343, <https://doi.org/10.5194/acp-23-1329-2023>, 2023.
- 770 Yu, L., Smith, J., Laskin, A., George, K. M., Anastasio, C., Laskin, J., Dillner, A. M., and Zhang, Q.: Molecular transformations of phenolic SOA during photochemical aging in the aqueous phase: competition among oligomerization, functionalization, and fragmentation, *Atmos. Chem. Phys.*, 16, 4511-4527, <https://doi.org/10.5194/acp-16-4511-2016>, 2016.
- 775 Zhang, G., Peng, X., Sun, W., Fu, Y., Yang, Y., Liu, D., Shi, Z., Tang, M., Wang, X., and Bi, X.: Fog/cloud processing of atmospheric aerosols from a single particle perspective: A review of field observations, *Atmos. Environ.*, 329, <https://doi.org/10.1016/j.atmosenv.2024.120536>, 2024a.
- [Zhang, X., Chen, Z. M., and Zhao, Y.: Laboratory simulation for the aqueous OH-oxidation of methyl vinyl ketone and methacrolein: significance to the in-cloud SOA production, *Atmos. Chem. Phys.*, 10, 9551-9561, <https://doi.org/10.5194/acp-10-9551-2010>, 2010.](https://doi.org/10.5194/acp-10-9551-2010)
- 780 Zhang, Y., Xu, W., Zhou, W., Li, Y., Zhang, Z., Du, A., Qiao, H., Kuang, Y., Liu, L., Zhang, Z., He, X., Cheng, X., Pan, X., Fu, Q., Wang, Z., Ye, P., Worsnop, D. R., and Sun, Y.: Characterization of organic vapors by a Vocus proton-transfer-reaction mass spectrometry at a mountain site in southeastern China, *Sci. Total Environ.*, 919, 170633, <https://doi.org/10.1016/j.scitotenv.2024.170633>, 2024b2024.
- 785 Zhao, J., Qiu, Y., Zhou, W., Xu, W., Wang, J., Zhang, Y., Li, L., Xie, C., Wang, Q., Du, W., Worsnop, D. R., Canagaratna, M. R., Zhou, L., Ge, X., Fu, P., Li, J., Wang, Z., Donahue, N. M., and Sun, Y.: Organic Aerosol Processing During Winter Severe Haze Episodes in Beijing, *J. Geophys. Res.-Atmos.*, 124, 10248-10263, <https://doi.org/10.1029/2019jd030832>, 2019.
- Zhao, R., Lee, A. K. Y., Huang, L., Li, X., Yang, F., and Abbatt, J. P. D.: Photochemical processing of aqueous atmospheric brown carbon, *Atmos. Chem. Phys.*, 15, 6087-6100, <https://doi.org/10.5194/acp-15-6087-2015>, 2015.
- 790 [Zhao, Y., Hallar, A. G., and Mazzoleni, L. R.: Atmospheric organic matter in clouds: exact masses and molecular formula identification using ultrahigh-resolution FT-ICR mass spectrometry, *Atmos. Chem. Phys.*, 13, 12343-12362, <https://doi.org/10.5194/acp-13-12343-2013>, 2013.](https://doi.org/10.5194/acp-13-12343-2013)

Supplement of

Molecular composition and processing of aqueous secondary organic aerosol in ~~cloud~~clouds at a mountain site in southeastern China

Yali Jin et al.

5 *Corresponding to:* Defeng Zhao (dfzhao@fudan.edu.cn)

Text S1. Meteorological condition and backward trajectories

10 The temperature (T) of CE1 was the lowest ~~of~~among the four CEs, while the T of CE3 was the highest. In CE2, RH was
the highest in four CEs. The air mass of CE1 originated from the southwest of the Shanghuang site. The duration time of CE2
was 22.5 hours, during which the origin of air mass turned from southwest (Fujian and Jiangxi provinces) to north (Mongolia)
at 12:00 on May 12th, resulting in a marked decrease in PM_{2.5} concentration. CE3 lasted for 1.5 h, the shortest duration time,
so RH and T were more stable. The air mass in CE3 originated from the ocean in the southeast, which is different from other
15 CEs. The duration time of CE4 is 34 h, the longest of all CEs, the air mass of which came from the southwest and turned to
the northeast in the second half of the duration time at 17:00 on May 27th.

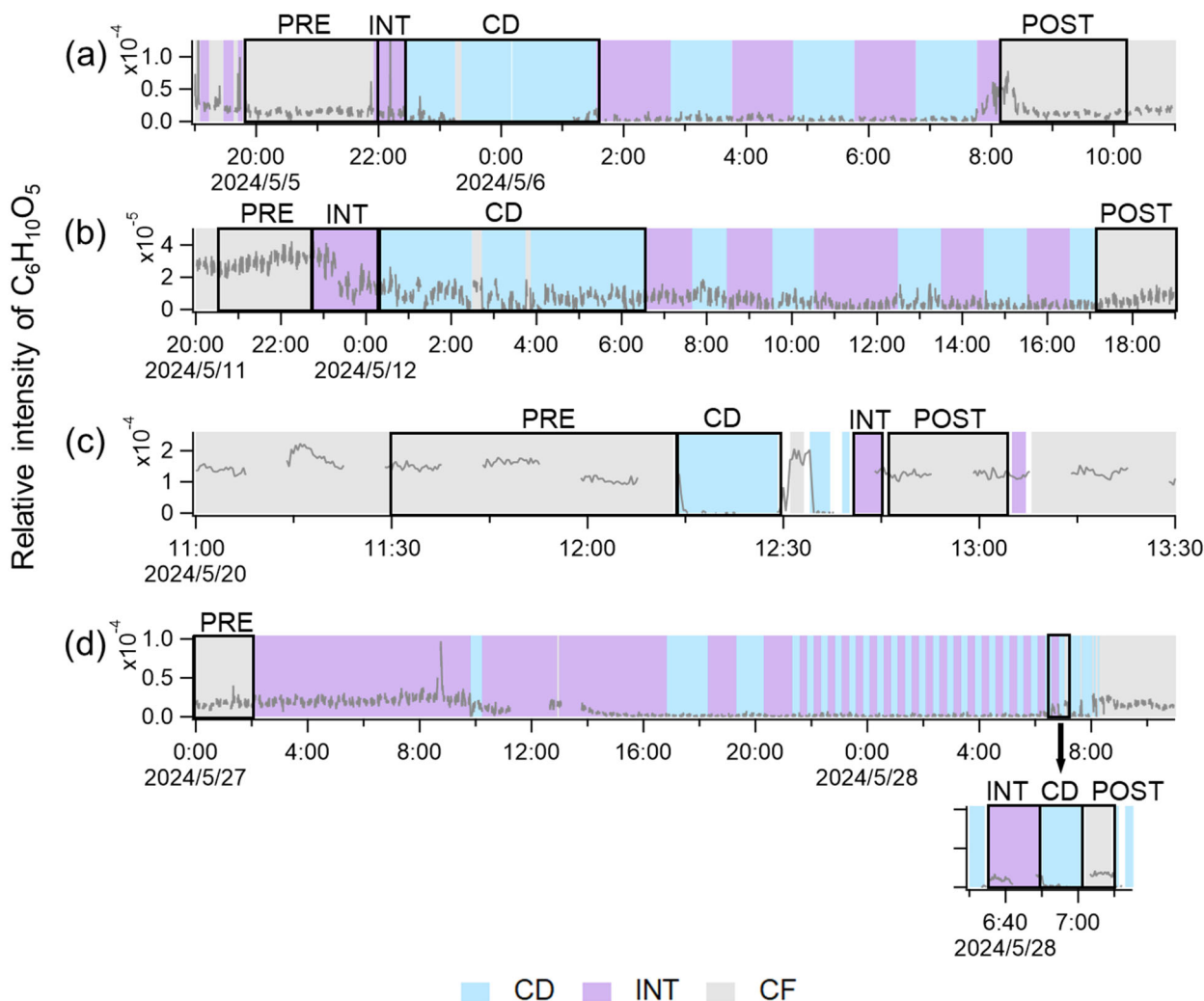
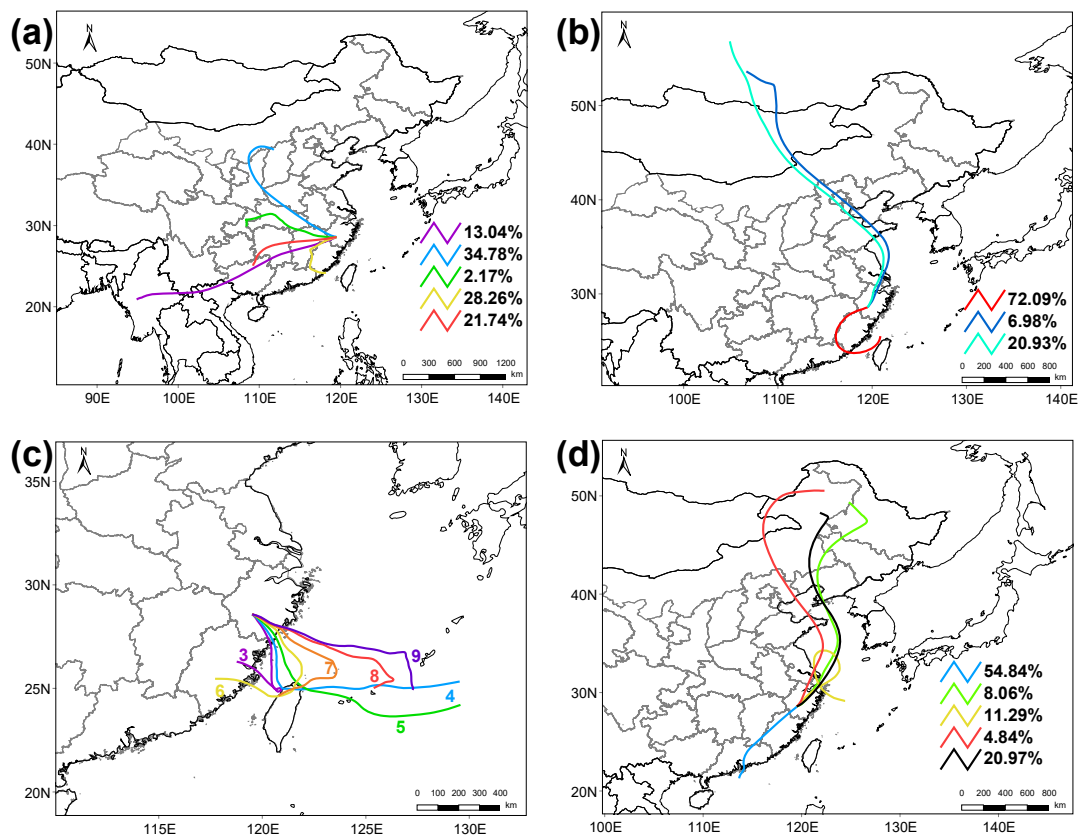


Figure S1. Operational definition of the pre-cloud, in-cloud (including sample types of CD and INT) and post-cloud stages in (a) CE1, (b) CE2, (c) CE3, and (d) CE4. Time series of $C_6H_{10}O_5$ is shown as an example. CD, INT, and CF samples are shaded in blue, purple, and gray, respectively. Gaps in the time series represent EESI-ToF-MS background measurement periods, which are not shown.



25

Figure S2. HYSPLIT 3-day backward trajectory analysis of air masses arriving at the Shanghuang site in (a) CE1, (b) CE2, (c) CE3, and (d) CE4. Trajectories are based on cluster analysis for CE1, CE2 and CE4. For CE3, due to its short duration, only 7-hour trajectories are shown with time in UTC.

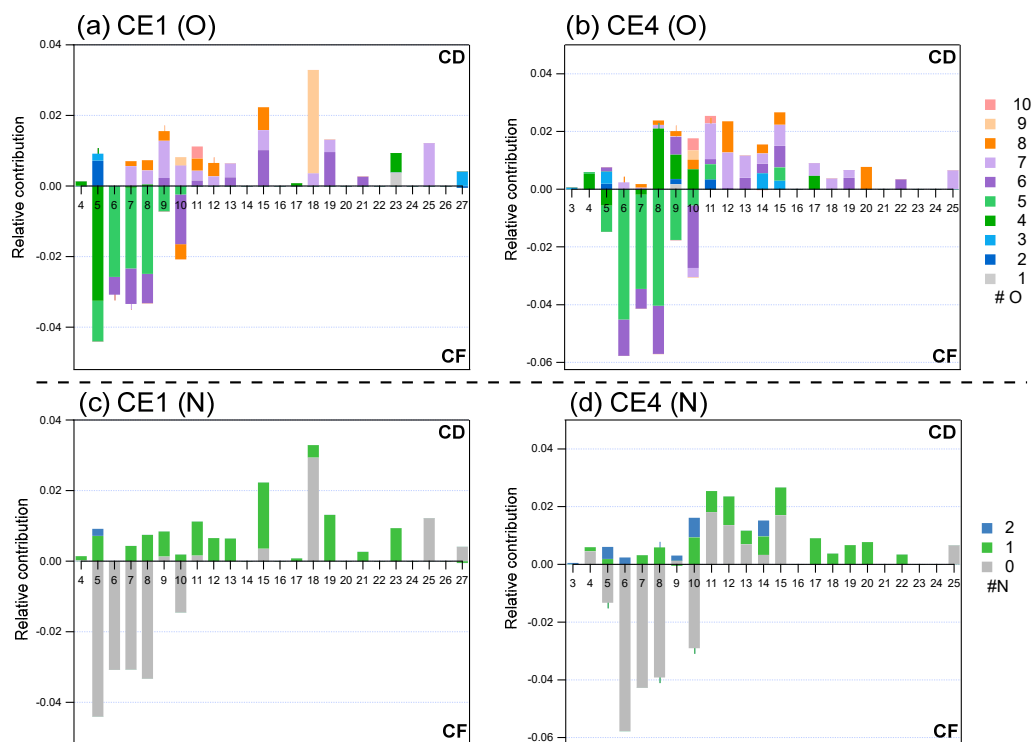


Figure S3. Detailed relative contribution of OA. The average carbon number distribution of differences between CD and CF are colored by oxygen number of CE2 (a), CE3 (b); and nitrogen number of CE2 (c), CE3 (d). Positive value stands for significant molecular characteristics of CD, and negative value stands for that of CF. Fractions of compounds are normalized to sum of signals of all organics in CD and CF, respectively.

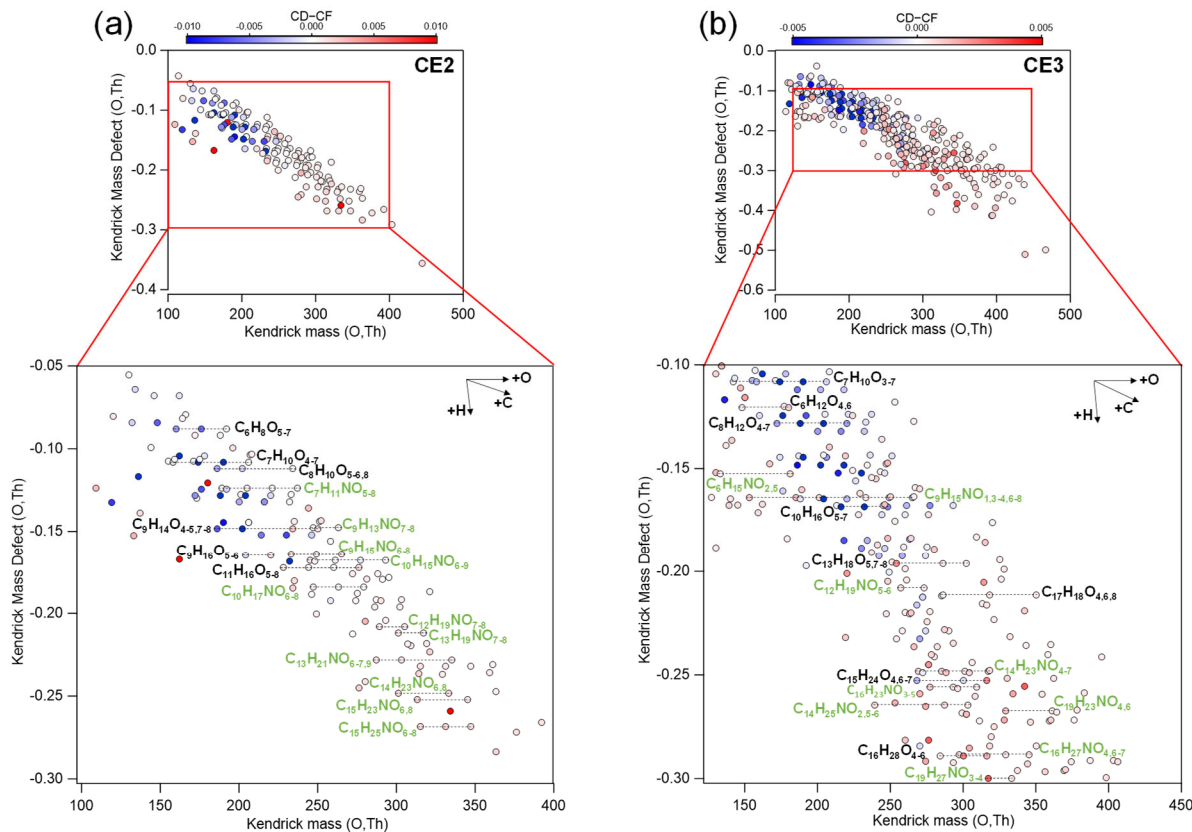
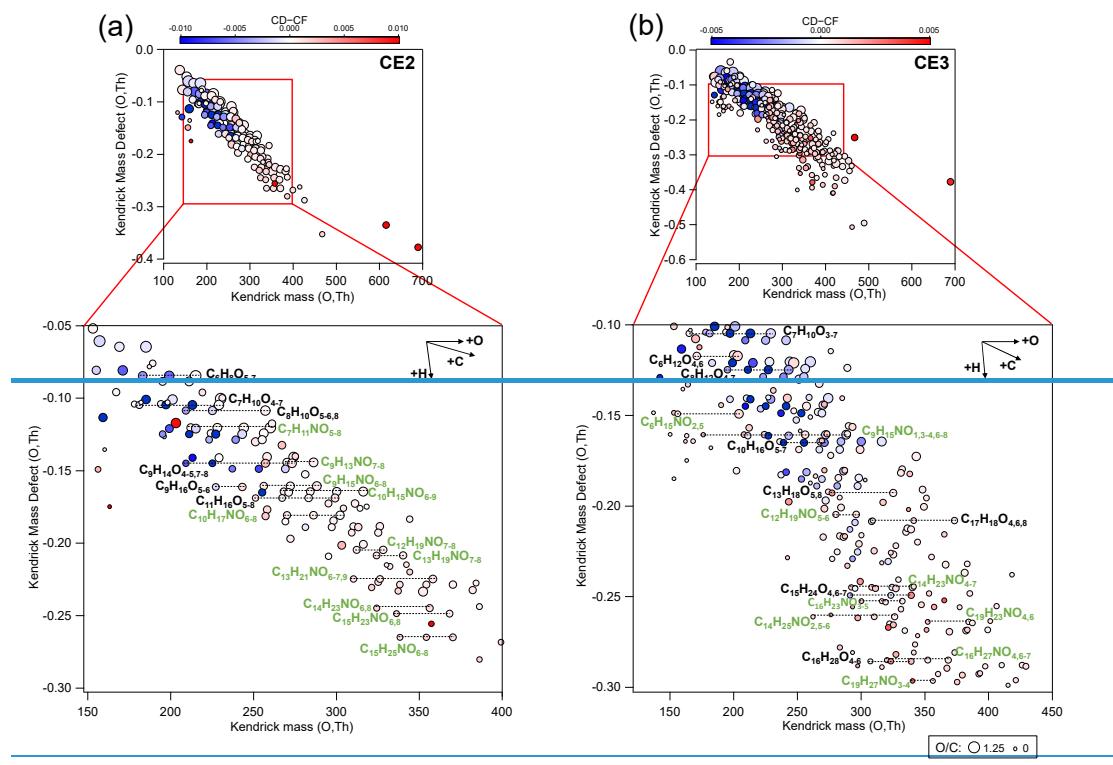


Figure S4. Kendrick mass defect **plots** based on O of compounds in (a) CE2 and (b) CE3. Data points are color-coded by differences **of** fin fraction of compounds between CD and CF **and sized by the O/C ratio**. Fraction of compounds are normalized to the sum of signals of all organics in CD and CF, respectively. Note that, for conciseness, data points in CE3 with normalized signal difference between -0.0003 and 0.0003 (appearing nearly white) are not shown here. **The molecular formulas include the reagent ion Na^+ , which is** **Siloxane compounds are not shown here for simplicity/clarity.**

40

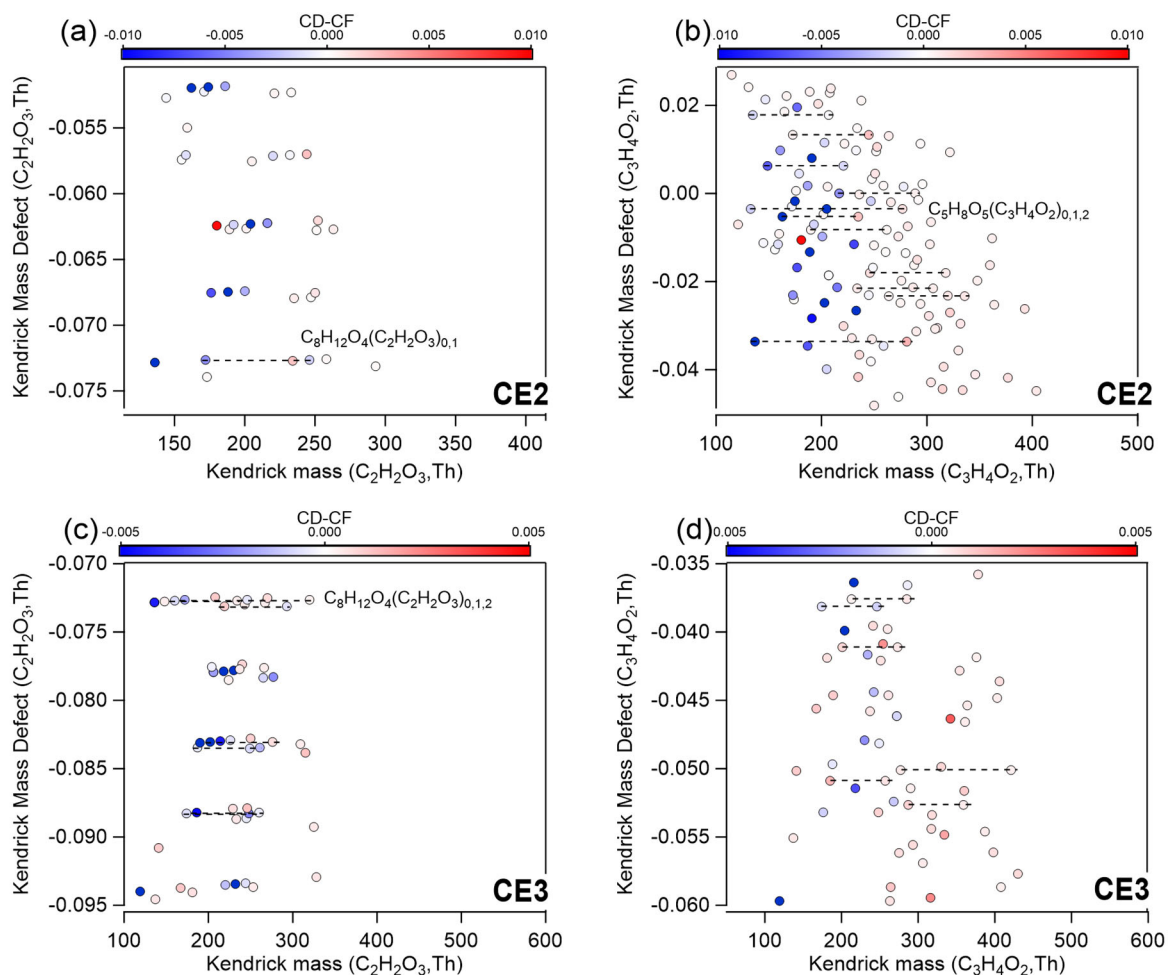
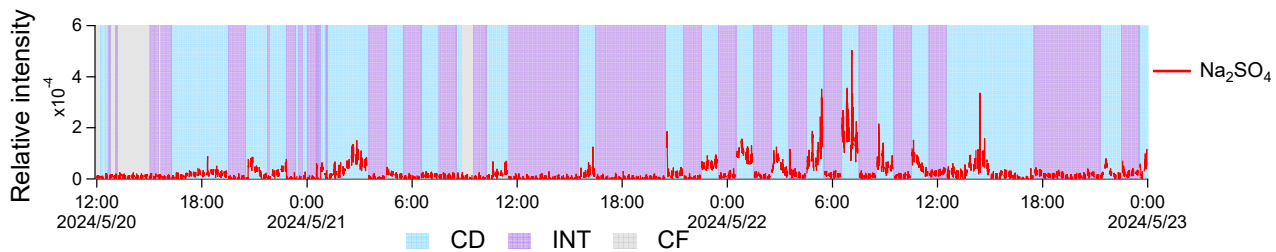


Figure S5. Kendrick mass defect plots based on (a) $C_2H_2O_3$ and (b) $C_3H_4O_2$ of compounds in CE2; and (c) $C_2H_2O_3$ and (d) $C_3H_4O_2$ of compounds in CE3. Data points are color-coded by differences in fraction of compounds between CD and CF. Fraction of compounds are normalized to the sum of signals of all organics in CD and CF, respectively. Note that, for conciseness, data points in CE3 with normalized signal difference between -0.0003 and 0.0003 (appearing nearly white) are not shown here.



55

Figure S6. Typical time series of sulfate (Na_2SO_4) in a cloud episode. CD, INT, and CF are shaded as blue, purple, and gray, respectively. Gaps in the time series represent EESI-ToF-MS background measurement periods, which are not shown.

60 **Table S1: General characteristics of CE1–CE4, including PM_{2.5} and CO concentration, meteorological parameters (RH and T), origin of air mass, and duration time of each whole cloud episode, respectively. Measured values are shown as mean ± standard deviation.**

	CE1	CE2	CE3	CE4
PM _{2.5} (μg m ⁻³)	4.3±3.0	5.3±6.7	13.5±1.5	3.8±3.6
CO (ppm)	0.29±0.03	0.26±0.06	0.17±0.002	0.19±0.03
RH (%)	94.7±12.0	97.7±6.7	90.8±5.9	95.0±9.1
T (°C)	15.1±1.7	15.7±3.0	18.0±0.6	17.3±4.0
Origin of air mass	Southwest	Southwest then turns to north	Southeast	Southwest then turns to northwest
Duration time (hour)	14	22.5	1.5	34

65

Table S2: Mean atom numbers (n_C , n_H , n_O , and n_N ; mean \pm standard deviation) of OA for CE1–CE4 in pre-cloud aerosols, CD, INT, and post-cloud aerosols.

		Pre-cloud aerosols	CD	INT	Post-cloud aerosols
<u>CE1</u>	n_C	<u>8.72\pm0.38</u>	<u>10.45\pm1.07</u>	<u>8.99\pm0.53</u>	<u>8.86\pm0.41</u>
	n_H	<u>13.81\pm1.09</u>	<u>17.25\pm3.16</u>	<u>14.21\pm1.17</u>	<u>14.45\pm1.10</u>
	n_O	<u>5.64\pm0.12</u>	<u>6.02\pm0.33</u>	<u>5.68\pm0.13</u>	<u>5.71\pm0.15</u>
	n_N	<u>0.20\pm0.03</u>	<u>0.32\pm0.08</u>	<u>0.26\pm0.05</u>	<u>0.22\pm0.04</u>
<u>CE2</u>	n_C	<u>8.33\pm0.20</u>	<u>10.13\pm1.26</u>	<u>8.52\pm0.34</u>	<u>11.12\pm0.55</u>
	n_H	<u>13.72\pm0.65</u>	<u>19.51\pm4.50</u>	<u>14.19\pm1.05</u>	<u>21.10\pm2.80</u>
	n_O	<u>4.98\pm0.12</u>	<u>5.44\pm0.57</u>	<u>4.92\pm0.18</u>	<u>6.26\pm0.20</u>
	n_N	<u>0.28\pm0.04</u>	<u>0.39\pm0.09</u>	<u>0.33\pm0.07</u>	<u>0.33\pm0.07</u>
<u>CE3</u>	n_C	<u>10.57\pm0.18</u>	<u>12.92\pm0.70</u>	<u>10.42\pm0.09</u>	<u>10.51\pm0.13</u>
	n_H	<u>16.14\pm0.30</u>	<u>21.78\pm1.76</u>	<u>16.21\pm0.20</u>	<u>16.18\pm0.29</u>
	n_O	<u>5.08\pm0.05</u>	<u>5.15\pm0.12</u>	<u>5.09\pm0.03</u>	<u>5.11\pm0.04</u>
	n_N	<u>0.30\pm0.02</u>	<u>0.42\pm0.06</u>	<u>0.27\pm0.02</u>	<u>0.27\pm0.02</u>
<u>CE4</u>	n_C	<u>8.17\pm0.15</u>	<u>9.95\pm0.49</u>	<u>8.94\pm0.20</u>	<u>8.77\pm0.12</u>
	n_H	<u>12.99\pm0.19</u>	<u>14.53\pm0.65</u>	<u>13.36\pm0.26</u>	<u>13.20\pm0.17</u>
	n_O	<u>5.29\pm0.08</u>	<u>5.68\pm0.23</u>	<u>5.52\pm0.08</u>	<u>5.52\pm0.06</u>
	n_N	<u>0.12\pm0.03</u>	<u>0.32\pm0.08</u>	<u>0.20\pm0.04</u>	<u>0.18\pm0.02</u>

Table S3: Compounds with larger fraction in CD than CF in CE1, CE2, CE3, and CE4.

	Formula				
CE1	C4H4NO4	C8H13NO7	C10H17NO6	C15H23NO8	
	C4H6O5	C8H13NO8	C10H17NO7	C15H25NO8	
	C5H13NO2	C8H14O6	C11H16O6	C17H13NO4	
	C5H8N2O3	C9H12O6	C11H17NO7	C18H19NO7	
	C5H12O4	C9H12O7	C11H19NO8	C18H23NO7	
	C6H4O5	C9H13NO7	C11H23NO10	C18H54O9Si9	
	C6H10O6	C9H14O7	C12H19NO7	C19H25NO7	
	C7H8O5	C9H15NO7	C12H19NO8	C19H23NO6	
	C7H8O6	C9H15NO8	C13H15NO6	C21H31NO6	
	C7H10O7	C10H13NO8	C13H19NO7	C23H17NO	
	C7H11NO7	C10H14O7	C15H25NO6	C23H21NO4	
	C7H11NO8	C10H15NO7	C15H25NO7	C25H32O7	
	C8H6O4	C10H15NO8	C15H15O6	C27H20O3	
	C8H10O6	C10H15NO9	C15H15NO7		
	C8H11NO7	C10H16O7	C15H23NO6		
	CE2	C3H2N2O3	C9H8O5	C11H18O6	C14H23NO6
C4H4NO4		C9H12O6	C11H19NO8	C14H23NO8	
C4H8O4		C9H13NO7	C11H20O8	C15H19NO6	
C6H8O7		C9H13NO8	C11H23NO10	C15H25NO6	
C6H9NO7		C9H14O7	C12H12O6	C15H25NO7	
C6H12O6		C9H14O8	C12H16O7	C15H15O6	
C6H15NO2		C9H15NO6	C12H16O8	C15H15NO7	
C7H8O5		C9H15NO7	C12H17NO7	C15H17N3O5	
C7H8O6		C9H15NO8	C12H17NO8	C15H21NO9	
C7H11N		C9H16O6	C12H18O7	C15H22O7	
C7H11NO5		C9H17NO6	C12H18O8	C15H23NO6	
C7H11NO6		C10H8O5	C12H19NO7	C15H23NO8	
C7H11NO7		C10H12O7	C12H19NO8	C15H25NO8	
C7H11NO8		C10H15NO6	C12H24O7	C16H19NO6	
C7H11N3		C10H15NO7	C13H19NO8	C16H48O8Si8	
C7H13N2SO		C10H15NO9	C13H15NO6	C17H13NO4	
C8H6O4		C10H14N2	C13H18O7	C17H22N2O5	
C8H10O8		C10H17NO6	C13H18O8	C18H19NO7	
C8H11NO5		C10H17NO7	C13H19NO7	C18H21NO7	
C8H11NO7		C10H17NO8	C13H20O6	C18H54O9Si9	
C8H14O6		C10H18O6	C13H21NO6	C19H17NO3	
C8H13NO7		C10H19NO6	C13H21NO7	C19H25NO6	
C8H13NO8		C11H14O7	C13H21NO9	C20H24O7	
C8H14O6		C11H16O5	C13H24O6	C21H25NO7	
C9H7N2O		C11H16O7	C14H21NO7	C25H32O7	
C9H7N2O2		C11H16O8	C14H21NO8	C27H20O3	
C9H8SO		C11H17NO7	C14H21NO9		
CE3		C4H7NO3	C12H10O7	C15H22O5	C19H18O6
		C4H7N3O3	C12H13NO6	C15H22O4	C19H19NO2
		C4H8O4	C12H14O7	C15H24O7	C19H20O7
	C4H9N3O3	C12H15NO5	C15H26O6	C19H22O5	
	C5H10O4	C12H16O10	C15H26O6	C19H22O7	
	C5H12O4	C12H19NO5	C15H28O6	C19H23NO4	
	C5H10O4	C12H19NO6	C15H32O7	C19H23NO6	
	C6H4SO3	C12H21NO6	C16H23NO5	C19H24O7	

	Formula			
	C6H10O3	C12H24O7	C16H25NO5	C19H26O4
	C6H11NO5	C12H36O6Si6	C16H27NO4	C19H26O6
	C6H12O4	C13H12O5	C16H27NO6	C19H28O6
	C6H12O6	C13H14O5	C16H27NO7	C19H29O8
	C6H14N2	C13H14O6	C16H29NO5	C19H31NO6
	C6H14N2O	C13H15N3O7	C16H33NO6	C19H38O5
	C6H15NO2	C13H18O7	C16H15NO	C19H39NO4
	C6H15NO5	C13H17NO4	C16H19NO6	C20H29NO5
	C6H15N3O	C13H18O5	C16H22O4	C20H12N2
	C6H17N3O3	C13H18O8	C16H22O9	C20H14N2O2
	C7H10O3	C13H20O6	C16H23NO3	C20H22O5
	C7H11N3	C13H19NO6	C16H23NO4	C20H24O4
	C7H12O8	C13H22O7	C16H24O5	C20H24O6
	C7H15N2	C13H21NO6	C16H25NO8	C20H24O7
	C7H18N2	C13H22O5	C16H26O8	C20H30O10
	C8H15NO4	C13H24O6	C16H28O4	C20H32O9
	C8H4O3	C14H15NO7	C16H28O5	C20H35NO7
	C8H5NO4	C14H23NO7	C16H28O6	C20H36O5
	C8H7NO	C14H7NO4	C16H32O10	C21H21NO6
	C8H13O2	C14H14O4	C17H33NO4	C21H25NO7
	C8H13NO6	C14H16O4	C17H33NO5	C21H22O5
	C8H15N2	C14H16O5	C17H37N5	C21H23NO2
	C9H7NO2	C14H16N2O3	C17H11N	C21H25NO6
	C9H10O2	C14H19NO7	C17H18O6	C21H26O6
	C9H10O2	C14H20O8	C17H18O8	C21H26O8
	C9H13NO2	C14H21NO	C17H22O5	C21H27NO8
	C9H14O7	C14H22O4	C17H22N2O	C21H28O8
	C9H15NO	C14H23NO4	C17H22N2O5	C21H34O2
	C9H15NO3	C14H23NO5	C17H24O5	C21H38O5
	C9H15NO4	C14H23NO6	C17H26N2O	C22H33NO4
	C9H15NO6	C14H24O6	C17H27NO3	C22H26O5
	C9H16O	C14H24O7	C17H28O7	C22H34O7
	C9H19S	C14H25NO2	C17H29NO	C22H38O6
	C10H12O7	C14H25NO5	C17H29NO7	C23H39NO4
	C10H12N2O4	C14H25NO6	C18H25NO4	C23H22O5
	C10H13NO6	C14H26O5	C18H27NO5	C23H26O6
	C10H15NO4	C14H28O5	C18H29NO6	C24H29NO4
	C10H14N2	C14H28O4	C18H16O6	C24H28O5
	C10H20O5	C14H31N3O10	C18H20O6	C24H50O8
	C11H12O4	C15H21NO8	C18H22O5	C25H17NO4
	C11H16O5	C15H25NO5	C18H23N	C26H29O6
	C11H16O8	C15H12O3	C18H27NO7	C26H29NO
	C11H17NO6	C15H11NO2	C18H28O7	C27H38O2
	C11H19NO6	C15H13N3O5	C18H35NO5	C27H50O4
	C11H20O6	C15H15NO2	C18H35N3O8	C28H24O2
	C11H20N2O5	C15H18O8	C18H54O9Si9	
	C11H21NO5	C15H19NO4	C19H27NO3	
	C11H21NO6	C15H20O4	C19H27NO4	
CE4	C3H2N2O3	C9H8SO	C11H16O5	C14H23NO8
	C4H4NO4	C9H8O5	C11H16O6	C15H25NO6
	C4H6O5	C9H10O6	C11H16O7	C15H25NO7

Formula			
C4H8O4	C9H12O6	C11H17NO7	C15H12O3
C5H13NO2	C9H12O4	C11H18O6	C15H15O6
C5H6O5	C9H12O7	C11H23NO10	C15H20O5
C5H6O6	C9H13NO7	C12H16O7	C15H22O7
C5H8N2O3	C9H13NO8	C12H16O8	C15H23NO6
C5H10O4	C9H14O8	C12H17NO7	C15H23NO8
C5H12O4	C9H16O6	C12H18O6	C15H25NO8
C6H10N2O7	C10H8O5	C12H18O7	C17H13NO4
C7H8O6	C10H12N2O4	C12H18O8	C17H19NO7
C7H10O7	C10H13NO8	C12H19NO7	C18H19NO7
C7H11NO6	C10H15NO6	C12H19NO8	C18H21NO7
C7H11NO8	C10H15NO7	C12H24O7	C18H23NO7
C7H12O6	C10H15NO8	C13H12O6	C19H25NO7
C8H12O4	C10H15NO9	C13H18O7	C19H23NO6
C8H14O5	C10H17NO6	C13H19NO7	C20H31NO8
C8H14O6	C10H17NO7	C13H20O6	C20H33NO8
C8H13NO7	C10H18O5	C14H15NO7	C22H25NO6
C8H13NO8	C10H20O10	C14H21NO8	C25H32O7
C8H14O6	C11H9NO2	C14H16N2O3	
C9H7N2O2	C11H14O7	C14H20O6	

Note: Duplicated molecular formulas originate from different ion adducts from the ionization of EESI-~~TOFT~~ToF-MS.